$^{40}Ar/^{39}Ar$ age determinations of four plutons associated with mineral deposits in southwestern New Mexico

Virginia T. McLemore, William C. McIntosh, and Tim C. Pease

Openfile Report 410

New Mexico Bureau of Mines and Mineral Resources
Socorro, NM 87801

December 1995

TABLE OF CONTENTS

INTRODUCTION

During examination of mineral resources in southwestern New Mexico, four plutons and one pegmatite were sampled for age determinations by $^{40}Ar/^{39}Ar$ methods: Animas quartz monzonite (Animas Mountains), Sugarloaf Peak quartz monzonite and associated Quickstrike pegmatite (Organ Mountains), Hanover-Fierro stock (Continental mine), and Granite Gap pluton (Peloncillo Mountains) (Table 1). These samples, representing relatively fresh outcrops of the intrusive rocks, were collected because of proximity to and possible association with known mineralization, existing discrepancy of published age determinations and/or locations of dated samples (Table 2), and large errors in published age dates that are inherent to conventional K-Ar techniques.

The purpose of this report is to provide age determinations of the intrusives, to discuss the relationship to known mineralization, and to better constrain the age of mineralization. In addition, cooling histories of some of the four plutons can be obtained from age determinations of biotite, hornblende, and K-feldspar. Brief descriptions of the areas are presented here and more detailed reports are in preparation.

Location, descriptions, and $^{40}Ar/^{39}Ar$ results from these samples are summarized in Table 1 and located in Figure 1. Published age determinations are in Table 2. The spectra and raw data are in Appendix 1.

Table 1—Location, description, and summary of $^{40}Ar/^{39}Ar$ age determinations.

Pluton	Sample	Latitude, Longitude	Lithology	District and associated mineralization	Mineral	Lab No.	Spectra			Isochron						Comments
							N	Age	Error	N	Age	Error	MSWD	40/36	Error	
Animas quartz monzonite	VM94-13	32°44'10", 108 41' 35"	quartz monzonite	Rincon manganese veins	biot	1207	4	33.58	0.12	9	33.70	0.12	9.95	287.0	1.7	Good spectrum
Sugarloaf Peak quartz monzonite	VM94-3	32°26' 10", 106°35' 00"	quartz monzonite	Organ district carbonate hosted Pb-Zn	biot hnbl Kfsp	1208 1209 1212	4 23	33.063 38.76	0.052 0.1	8 9 6	33.12 34.66 31.8	0.1 0.21 0.01	3.43 38.37 37.01	293.0 314.6 417.4	1.2 1.4 5.3	Good plateau Poor spectrum Excess Ar
Quickstrike pegmatite	Quick-6	32°26' 15", 106°33' 15"	pegmatite	Organ district pegmatite	Kfsp	1210	9	30.8	0.1	9	30.85	0.09	20.32	297.9	1.7	Rising spectrum
Hanover-Fierro stock	COB-4	32°50' 20", 108°5' 00"	quartz monzonite to granite to granodiorite	Fierro-Hanover (Continental mine)	biot Kfsp Kfsp	1851 1848 1848	8 10 5	57.55 57.03 57.39	0.07 0.05 0.07	8	57.52	0.06	0.95	449.8	138.7	Good plateau 950-1250°C steps 1300-1550° steps
Granite Gap pluton	GG	32°5' 20", 109°58' 25"	quartz monzonite to granite	Granite Gap carbonate hosted Pb-Zn	biot Kfsp	1850 1849	6 9	33.20 30.9	0.2 0.2	6	33.77	0.11	38.08	248.4	9.3	Fair spectrum Poor mineral separation

Table 2—Published age determinations of the four plutons. * Latitude, longitude not published and exact location of samples dated is uncertain.

Pluton	K-Ar date	Mineral	Latitude	Longitude	Reference
Animas quartz monzonite	34.83 ± 0.78	biotite	31°43'	108°48'	Deal et al. (1978)
Sugarloaf Peak quartz monzonite	32.8 ± 0.5	biotite	32°25'	106°34'	Loring and Loring (1980)
quartz-feldspar sill	34.4 ± 1.1	muscovite	32° 26'	106° 35'	
latite porphyry dike	32.1 ± 1.1	hornblende	32° 26'	106° 35'	
latite porhyry dike	32.9 ± 1.2	biotite	32° 26'	106° 35'	
Hanover-Fierro stock (granodiorite)	70.4 ± 2.1	hornblende	*	*	McDowell (1971)
	57.1 ± 2.0	biotite			
	67.2 ± 2.9	hornblende			
	58.0 ± 1.8	biotite			
	58.4 ± 1.8	hornblende			
Granite Gap granite	32.5 ± 1.0	biotite	32° 6' 24"	108° 58' 59"	Hoggatt et al. (1977)
	30.3 ± 0.9	biotite	32° 6' 23"	108° 59' 28"	
	31.8 ± 1.0	biotite	32° 5' 33"	108° 57' 59"	
	32.1 ± 1.0	plagioclase	32° 5' 33"	108° 57' 59"	
	29.8 ± 0.9	K-feldspar	32° 5' 33"	108° 57' 59"	
	33.0 ± 1.1	biotite	32° 5' 35"	108° 58' 00"	Marvin et al. (1978)
	32.9 ± 1.1	biotite	32° 5' 10"	108° 58' 50"	

BRIEF GEOLOGIC DESCRIPTIONS OF SAMPLE AREAS

Animas Mountains

The Animas quartz monzonite is one of several Tertiary plutons exposed in the Animas Mountains in Hidalgo County (Fig. 1). The oldest rocks in the Animas Mountains are Proterozoic granite (1200 Ma; Soulè, 1972; Drewes, 1986), which is unconformably overlain by Paleozoic marine and Cretaceous clastic sedimentary rocks. Tertiary volcanic and intrusive rocks form much of the range. The Rincon (or Animas) mining district lies in the Animas Mountains and consists of carbonate-hosted lead-zinc, carbonate-hosted manganese, and volcanic-epithermal veins. Production from the district has been minor, amounting to approximately $320,000 worth of copper, silver, gold, and lead and an unknown amount of manganese. The largest mines in the district consist of the Rincon, Fredingbloom, Zinc, White Rose, and Cowboy mines. A number of volcanic-epithermal manganese veins cut altered Animas quartz monzonite in the northern portion of the mountain range. The district has remained idle since the 1960s. Relatively unaltered Animas quartz monzonite was sampled from an arroyo north of the Rincon district

(Table 1). An altered sample of the pluton was previously dated as 34.83±0.78 Ma by K-Ar on biotite (Table 2; Deal et al., 1978).

Organ Mountains

The Organ Mountains, near Organ, Doña Ana County, form a west-tilted block exposing rocks that range in age from Proterozoic through Quaternary. Most of the range consists of the Organ batholith, which has been dated by K–Ar as 32.8 ± 0.5 Ma (Table 2; Loring and Loring, 1980). The Organ batholith is a complex pluton made up of multiple intrusions (Seager, 1981; Seager and McCurry, 1988); three major phases are the granite of Granite Peak (youngest), Sugarloaf Peak quartz monzonite and Organ Needle quartz syenite (oldest). All three phases are related to mineral deposits. Several dikes north of Organ intruding the Sugarloaf Peak quartz monzonite were also dated, and some of these dikes had age dates that were older than the age date obtained of the older pluton (32.1-34.4, Table 2). Therefore, relatively unaltered samples of the Organ batholith (Sugarloaf Peak quartz monzonite along US–70 at San Augustin Pass), rhyolite dikes north of Organ, and a pegmatite north of US–70 at San Augustin pass were collected. Only the samples of the batholith and pegmatite were analyzed (Table 1); the rhyolite dikes were fine-grained and feldspar separates could not be easily obtained.

The Organ Mountains mining district forms much of the Organ Mountains. Metal production from the district amounts to $2.7 million worth of copper, lead, zinc, silver and gold. This district is the 6th largest producing lead district in New Mexico with approximately 25 million pounds of lead produced from 1849 to 1961. Approximately 1.7 million pounds of zinc were also produced (McLemore and Lueth, 1995). Other production from the Organ Mountains district amounts to 600 tons of barite; 1,650 tons of fluorite; 14 pounds of uranium; and 9 pounds of vanadium. Bismuth occurs locally; a small amount was produced from the Texas Canyon mine (Dasch, 1965) and other ore shipments were penalized for bismuth at the smelter. Uranium and barite were produced from the Bishops Cap area (Williams et al., 1964; McLemore, 1983). There has been no production since 1961.

Six types of deposits are found in the Organ Mountains district and form five metal zones (Fig. 2; Dunham, 1935; Seager, 1981; Seager and McCurry, 1988; McLemore and Lueth, 1995). Copper-molybdenum mineralization forms a core, surrounded by zinc-lead, lead-zinc, gold-silver, and outer fluorite-barite zones (Fig. 2). This district-wide zoning is best preserved in the northern Organ Mountains where disseminated copper and molybdenum mineralization has been encountered in drill holes northwest of Organ and may represent a faulted portion of a copper-molybdenum porphyry deposit (Newcomer and Giordano, 1986). A zone of disseminated and veined pyrite occurs to the east at San Augustin Pass in the Sugarloaf Peak quartz monzonite, the most volatile-rich phase of the Organ batholith, and forms the center of the northern part of the district. Silver-bearing pegmatites (sample, Quick-6) occur near San Augustin Pass in the Sugarloaf Peak quartz monzonite (Dunham, 1935). Copper-breccia deposits occur west of the Sugarloaf Peak quartz monzonite at the Torpedo and Memphis mines. A transition from disseminated copper and molybdenum to copper skarns and breccias to zinc-lead skarns and replacement deposits occurs in carbonates northwest of the Memphis mine and near the Excelsior mine in the northern portion of the district (Lueth, 1988). The Homestake and Memphis deposits are zinc-lead skarns. The Merrimac mine is predominantly zinc replacements; lead with silver becomes more dominant to the east. The Hilltop and Black Prince mines are predominantly carbonate-hosted lead-silver deposits. The Stevenson-Bennett is a carbonate-hosted lead-silver and zinc-lead deposit. Gold and silver epithermal/mesothermal veins occur in the Proterozoic rocks in the Gold Hill area, east of the Sugarloaf Peak quartz monzonite (Fig. 2). Silver decreases to the north and barite becomes dominant. The Modoc and Orejon deposits along the west side of the Organ Mountains are lead-zinc skarn and replacement deposits and may be related to a third copper-molybdenum zone in the central Organ Mountains near Organ Peak.(Fig. 2). An outer zone, surrounding the Organ Mountains batholith, consists of sedimentary-hydrothermal barite-fluorite deposits, locally with copper, lead, silver, uranium, and vanadium; examples include the Bishops Cap and Ruby mines.

Fierro-Hanover district

The Fierro-Hanover mining district is approximately 12 miles east-northeast of Silver City and was discovered in 1850. From 1890 to 1980s, 1.25 billion lbs Cu, >50,000 oz Au, >5 million oz Ag, >52 million lbs Pb, and 1.21 billion lbs Zn were produced. The district is the largest zinc producing district and 4th largest lead producing district in New Mexico (McLemore and Lueth, 1995). Mineral deposits in the district consist of large polymetallic-skarn, carbonate-hosted lead-zinc vein and replacement, small replacement manganese, and iron-skarn deposits in steeply-dipping fracture zones in Paleozoic limestones. The Continental mine is currently producing copper with reported reserves of 10,300,000 tons of 0.92% Cu (open-pit), 3,600,000 tons of 2.3% Cu (underground), and 80,000,000 tons of 0.38% Cu as acid-leachable chalcocite (Hillesland et al., 1994, 1995).

The Fierro-Hanover district is centered around the Hanover-Fierro pluton, a north-trending elongate, discordant intrusion about 1 km wide and 4 km long, which intrudes Upper Cambrian to Cretaceous sedimentary carbonate and clastic rocks. The pluton consists of light gray, fine- to coarse-grain granodiorite porphyry. A relatively unaltered sample of the granodiorite porphyry was obtained from the north side of the Continental south pit (Table 1; elevation 6680 ft). The Barringer fault is a major fault and cuts the Continental deposit. The Fierro-Hanover district is one of the most strongly zinc mineralized areas in New Mexico (Fig. 3). Proximal Zn-Pb skarns occur around the southern lobe of the Hanover-Fierro pluton and distal Pb-Zn skarns occur along faults and dikes throughout the area (Jones et al., 1967; Meinert, 1987; Lueth, 1984). The skarns are typically zoned (Fig. 3); garnet replacement bodies occur nearest the pluton grading outwards to clinopyroxene-garnet and clinopyroxene zones. Base-metal zoning is generally observed with copper associated with garnet and clinopyroxene-garnet skarn zones nearest the pluton and lead-zinc in the outer clinopyroxene zone.

Peloncillo Mountains

The Granite Gap (or San Simon) mining district is located near the southern end of the central Peloncillo Mountains east of the Arizona-New Mexico state line and southwest of Lordsburg. The oldest rocks in the district are Precambrian granite that crops out in a northwest-trending band in the northern part of the district, north of Preacher Mountain. Much of the remainder of the district consists mainly of Cretaceous and Paleozoic marine sedimentary rocks exposed in fault-bounded blocks. A large area in the southern part of the district, on either side of Granite Gap, has been intruded by the Granite Gap granite (Cargo, 1959; Armstrong et al., 1978; Gebben, 1978; Richter et al., 1990). The granite is located mostly between Preacher Mountain and Granite Gap faults. Previously, Gillerman (1958) describes this granite as being Precambrian and part of a fault-bounded horst trending east-northeast transversing across the middle of the mountain range at Granite Gap. Seven age dates are reported in the literature ranging from 29.8 to 32.9 Ma (Table 2). A sample was collected along the highway at Granite Gap (Table 1).

Deposits in the district were first explored in about 1887 (Gillerman, 1958). Carbonate-hosted lead-zinc replacement deposits occur peripheral to the granite. Most production ended in 1915, although small amounts of ore were produced sporadically until 1926 and probably into the 1950s. Total estimated production from the district amounts to $1.95 million, including more than 1.6 million lbs Pb and 91,000 oz Ag. In addition, 300 short tons of 0.5% WO_3 was produced in 1943. There is no current production.

ANALYTICAL PROCEDURES

Samples were collected, crushed, and sieved. K-feldspars were separated by magnetic and heavy-liquid techniques from the 250-300 micrometer size fraction. Biotites and hornblendes were hand-picked on the basis of color and shape. All mineral separates were washed with distilled water. Hornblende and K-feldspar separates were treated by ultrasound for 3-5 minutes to clean off any phases clinging to the grain margins. All flux monitors and samples were placed in Al-foil packets and packed into evacuated quartz vials. Samples of flux monitor, Fish Canyon Tuff (age = 27.84 Ma relative to 520.9 Ma for Mmhb-1; Samson and Alexander, 1981) were placed at intervals between unknowns. Samples were irradiated in the L67 position of the University of Michigan Ford Reactor for a period of ten hours. After irradiation, flux monitor samples were placed into a copper laser tray, four grains per hole, four holes per sample packet. The laser tray was placed under vacuum in the laser extraction line. The unknown samples were placed under vacuum in the furnace section of the extraction line. The NMGRL (New Mexico Geochronological Laboratory) system is typically pumped down to a pressure of 10^{-9} Torr, following bake out at approximately 150°C.

Flux monitor samples were fused with a 10W carbon dioxide laser for 20 seconds, then reactive gasses were removed by a SAES GP–50 getter operated at 0.2A. Scrubbed gas was then analyzed by the MAP–215–50 mass spectrometer using the electron multiplier (normal ^{40}Ar sensitivity of 2 x 10^{-17}

moles/pA). J-factors were calculated to a precision of ± 0.25% by averaging results of the four samples of each monitor.

Unknown samples were analyzed in a Tantalum double-vacuum resistance furnace which has temperature control accurate to ± 10°C. Samples were heated using 10- to 12-step heating schedules programmed into the system. After reactive gasses were removed by AP–10 and GP–50 SAES getters, the unknown samples were analyzed by the MAP–215–50 in the same manner as the flux monitors. ^{40}Ar blanks over the course of the analysis ranged from 10^{-16} to 10^{-15} moles. Uncertainties for ages are quoted at the one-sigma level. All ages have been calculated with the decay constants and isotope abundances recommended by Steiger and Jager (1977).

RESULTS AND INTERPRETATIONS

Animas Mountains

The VM94-13 biotite from the Animas quartz monzonite yields a spectrum dominated by a flat segment averaging 33.6 ± 0.1 Ma (Fig. 4), which is in agreement with the isochron age of 33.7 ± 0.1 Ma (Table 1). The biotite age of **33.6 ± 0.1 Ma** is considered to be the best estimate for when the pluton cooled through the biotite closure temperature of ~300 °C. The epithermal manganese veins cutting the pluton are therefore younger than 33.6 Ma.

Organ Mountains

The VM94-3 biotite from the Sugarloaf Peak quartz monzonite yielded a flat spectrum with a well defined plateau at 33.1 ± 0.1 Ma (Fig 5). The VM94-3 K-feldspar yielded a saddle-shaped spectrum, with flat segments centered at approximately 33 and 41 Ma (Fig. 6). The shape of the age spectrum, which is in part older than the biotite plateau, indicate excess Ar in this K-feldspar. The VM94-3 hornblende yielded a disturbed age spectrum (Fig 7). Low radiogenic yields coupled with anomoulously high K/Ca ratios indicate alteration and/or contamination by K-bearing phases. The biotite age of **33.1 ±**

0.1 Ma is considered the best estimate for when the pluton cooled through the biotite closure temperature of ~300 °C.

The Quick-2 K-feldspar from the Quickstrike pegmatite yielded a rising spectrum with flat segments averaging **30.8 ± 0.1 and 32.2 ± 0.1 Ma** (Fig 8). The form of the spectrum suggests that the K-feldspar may have closed at 32.5 Ma and was reheated and partially reset at 30.8 Ma. The younger age may indicate that hydrothermal fluids were mobile at that time and reset the age date. The isochron plot for the steps E - M (Table 1) yields an age of 30.8 ± 0.1 Ma, which agrees with the weighted mean average for those steps, although the MSWD (mean standard weighted deviation) of the isochron is high (20.4). The $^{40}Ar/^{36}Ar$ for those steps is close to atmospheric (Table 1), suggesting no trapped ^{40}Ar component is present. The maximum age of the mineral deposits in the Organ Mountains is 33.1 Ma; mineralization probably continued through at least 30.8 Ma.

Fierro-Hanover district

The COB-4 biotite from the Hanover-Fierro stock (Fig. 9) yielded a flat spectrum with a well defined plateau at 57.55 ± 0.07 Ma, and the COB-4 K-feldspar (Fig. 10) yielded a slightly rising spectrum with flat segments at 57.03 ± 0.05 Ma and 57.39 ± 0.07 Ma. These data are consistent with emplacement of the pluton and cooling through the closure temperature of biotite (~300°C) near **57.55 ± 0.07 Ma,** followed by cooling through the closure temperature range of K-feldspar (~250-150°C) between 57.03 ± 0.05 Ma and 57.39 ± 0.07 Ma. It follows that 57 Ma is the maximum possible age for the skarn deposits associated with the Hanover-Fierro stock.

Peloncillo Mountains

The GG biotite from the Granite Gap pluton (Fig. 11) yielded a moderately rising spectrum with a flat segment averaging **33.20 ± 0.20 Ma**. This age is the best estimate for the timing of emplacement and cooling of the pluton. The GG K-feldspar (Fig. 12) yielded small signals and a highly disturbed spectrum with a fairly flat segment at 30.9 ± 0.2 Ma. Signal size and K/Ca ratios clearly indicate that the mineral separate was not pure K-feldspar, so this age estimate is unreliable. The carbonate-hosted lead-zinc deposits associated with the Granite Gap pluton were emplaced after 33.2 Ma.

ACKNOWLEDGEMENTS—Thanks to the personel of the New Mexico Geochronological Laboratory, especially Matt Heizler, for analyzing the samples. This work is part of ongoing research of mineral resources in New Mexico at NMBMMR, Charles Chapin, Director and State Geologist.

References

Armstrong, A. K., Silberman, M. L., Todd, V. R., Hoggatt, W. C., and Carten, R. B., 1978, Geology of the central Peloncillo Mountains, Hidalgo County, New Mexico: New Mexico Bureau of Mines and Mineral Resources, Circular 158, 19 pp.

Cargo, D. N., 1959, Mineral deposits of the Granite Gap area, Hidalgo County, New Mexico: M.S. thesis, University of New Mexico, Albuquerque, 70 pp.

Dasch, M. D., 1965, Antimony, arsenic, bismuth, and cadmium; *in* Mineral and water resources of New Mexico: New Mexico Bureau of Mines and Mineral Resources, Bulletin 87, pp. 365–372.

Deal, E. G., Elston, W. E., Erb, E. E., Peterson, S. L., Reiter, D. E., Damon, P. E., and Shafiqullah, M., 1978, Cenozoic volcanic geology of the Basin and Range province in Hidalgo County, southwestern New Mexico; *in* Callender, J. J., Wilt, J., Clemons, R. E., and James, H. L., eds., Land of Cochise: New Mexico Geological Society, Socorro, Guidebook 29, pp. 219–230.

Drewes, H., 1986, Geologic map of the northern part of the Animas Mountains, Hidalgo County, New Mexico: U. S. Geological Survey, Miscellaneous Investigations Map I–686, scale 1:24,000.

Dunham, C. K., 1935, The geology of the Organ Mountains with an account of the geology and mineral resources of Doña Ana County, New Mexico: New Mexico Bureau of Mines and Mineral Resources, Bulletin 11, 272 pp.

Gebben, D. J., 1978, Geology of the central Peloncillo Mountains, the north third of the Pratt quadrangle, Hidalgo County, New Mexico: M. S. thesis, Western Michigan University, 126 pp.

Gillerman, E., 1958, Geology of the central Peloncillo Mountains, Hidalgo County, New Mexico, and Cochise County, Arizona: New Mexico Bureau of Mines and Mineral Resources, Bulletin 57, 152 pp.

Hillesland, L. L., Worthington, W. T., and Hawkins, R. B., 1994, General geology of the Continental mine, Grant County, New Mexico; *in* Trip 10 and 13; Tyrone, Piños Altos, Chino, Continental, Central district, New Mexico: Bootprints along the Cordillera, Field Guide, 22 pp.

Hillesland, L. L., Hawkins, R. B., and Worthington, W. T., 1995, The geology and mineralization of the Continental mine area, Grant County, New Mexico; *in* Pierce, F. W. and Bolm, J. G., eds., Porphyry copper deposits of the American Cordillera: Arizona Geological Society Digest 20, pp. 473–483.

Hoggatt, W. L., Silberman, M. L., and Todd, V. R., 1977, K–Ar ages of intrusive rocks of the central Peloncillo Mountains, Hidalgo County, New Mexico: Isochron/West, no. 19, pp. 3–6.

Jones, W. R., Hernon, R. M., and Moore, S. L., 1967, General geology of Santa Rita quadrangle, Grant County, New Mexico: U. S. Geological Survey, Professional Paper 555, 144 pp.

Loring, A. K., and Loring, R. B., 1980, K/Ar ages of middle Tertiary igneous rocks from southern New Mexico: Isochron/West, no. 28, pp. 17–19.

Lueth, V. W., 1984, Comparison of copper skarn deposits in the Silver City mining region, southwestern New Mexico: unpublished M. S. thesis, University of Texas at El Paso, 179 pp.

Marvin, R. F., Naeser, C. W., and Mehnert, H. H., 1978, Tabulation of radiometric ages including unpublished K-Ar and fission-track age for rocks in southeastern Arizona and southwestern New Mexico; *in* Callender, J.J., Wilt, J., Clemons, R.E., and James, H.L., eds., Land of Cochise: New Mexico Geological Society, Socorro, Guidebook 29, pp. 243–252.

McDowell, F. W., 1971, K-Ar ages of igneous rocks from the western United States: Isochron/West, no. 2, pp. 1–16.

McLemore, V. T., 1983, Uranium and thorium occurrences in New Mexico: distribution, geology, production, and resources, with bibliography: New Mexico Bureau of Mines and Mineral Resources, Open-file Report 183, 960 pp.

McLemore, V. T. and Lueth, V. W., 1995, Carbonate-hosted lead-zinc deposits in New Mexico (abstr.): International Conference on Carbonate-hosted lead-zinc deposits, Extended Abstracts, Society of Economic Geologists, pp. 209–211.

Meinert, L. D., 1987, Skarn zonation and fluid evolution in the Groundhog mine, Central mining district, New Mexico: Economic Geology, v. 82, pp. 523–545.

Newcomer, R. W., Jr., and Giordano, T. H., 1986, Porphyry-type mineralization and alteration in the Organ mining district, south-central New Mexico: New Mexico Geology, v. 8, no. 4, pp. 83–86.

Richter, D. H., Lawrence, V. A., Drewes, Harald, Young, T. H., Enders, M. S., Damon, P. E., and Thorman, C. H., 1990, Geologic map of the San Simon quadrangle and parts of the Summit Hills and Mondel quadrangles, Cochise, Graham, and Greenlee Counties, Arizona, and Hidalgo County, New Mexico: U. S. Geological Survey, Miscellaneous Investigations Series Map I–1951, scale 1:48,000.

Samson and Alexander, 1981

Seager, W. R., 1981, Geology of the Organ Mountains and southern San Andres Mountains, New Mexico: New Mexico Bureau of Mines and Mineral Resources, Memoir 36, 97 pp.

Seager, W. R. and McCurry, M., 1988, The cogenetic Organ cauldron and batholith, south-central New Mexico: Evolution of a large-volume ash-flow cauldron and its source magma chamber: Journal of Geophysical Research, v. 93, no. B5, pp. 4421–4433.

Soulé, J. M., 1972, Structural geology of Northern part of Animas Mountains, Hidalgo County, New Mexico: New Mexico Bureau of Mines and Mineral Resources, Circular 125, 15 pp.

Steiger, R. H., and Jager, E., 1977, Subcommission on geochronology: Convention on the use of decay constants in geo- and cosmochronology: Earth Planet Sci. Lett. v. 36, pp. 359–362.

Williams, F. E., Fillo, P. V., and Bloom, P. A., 1964, Barite deposits of New Mexico: New Mexico Bureau of Mines and Mineral Resources, Circular 76, 46 pp.

Run ID#	Temp	40/39	37/39	36/39	39K moles	K/Ca	Cl/K	%40*	%39Ar	Age	± Err
Animas K-feldspar											
VM94-13, K-spar, 10.0 mg J=0.0006727±0.000002											
1206-01B	500	6.31E+02	0.00E+00	1.21E+00	5.0E-17	#DIV/0!	1.5E-01	43.5	0.00	305.773	316.638
1206-01C	600	5.72E+02	9.14E-02	1.83E+00	1.3E-14	5.6E+00	6.3E-03	5.4	0.80	37.019	5.839
1206-01E	800	6.49E+01	2.91E-01	1.27E-01	1.0E-13	1.8E+00	2.6E-04	42.3	7.10	33.020	0.328
1206-01F	850	4.41E+01	1.84E-02	5.21E-02	5.2E-14	2.8E+01	6.4E-04	65.1	10.34	34.535	0.302
1206-01G	900	3.82E+01	1.78E-02	3.42E-02	7.9E-14	2.9E+01	2.7E-04	73.5	15.30	33.710	0.213
1206-01H	950	3.69E+01	1.77E-02	2.88E-02	8.4E-14	2.9E+01	3.2E-04	76.9	20.52	34.064	0.131
1206-01I	1000	3.76E+01	1.32E-02	3.15E-02	8.7E-14	3.9E+01	5.2E-05	75.2	25.93	33.952	0.213
1206-01J	1050	4.10E+01	1.02E-02	4.33E-02	9.5E-14	5.0E+01	2.2E-04	68.7	31.83	33.865	0.301
1206-01K	1100	4.61E+01	8.95E-03	6.26E-02	1.1E-13	5.7E+01	3.8E-04	59.8	38.74	33.194	0.174
1206-01L	1150	5.28E+01	7.29E-03	8.62E-02	1.6E-13	7.0E+01	4.0E-04	51.8	48.83	32.887	0.202
1206-01M	1200	5.96E+01	8.67E-03	1.10E-01	2.8E-13	5.9E+01	1.4E-04	45.4	66.42	32.520	0.171
1206-01N	1250	6.82E+01	7.83E-03	1.36E-01	2.1E-13	6.5E+01	1.8E-04	41.0	79.44	33.620	0.234
1206-01O	1300	6.60E+01	5.76E-03	1.25E-01	1.1E-13	8.9E+01	5.1E-04	44.1	86.04	34.965	0.276
1206-01P	1650	5.59E+01	7.61E-03	9.38E-02	2.2E-13	6.7E+01	1.2E-04	50.3	99.59	33.802	0.228
1206-01Q	1650	5.08E+01	4.01E-02	7.82E-02	6.6E-15	1.3E+01	2.9E-03	54.5	100.00	33.244	0.979
		total gas age	n=15		1.6E-12	#DIV/0!	#DIV/0!			33.522	0.280
Animas biotite											
VM 94-13; BIOT,4.5MG, J=0.0006718±0.000002											
1207-01B	630	7.81E+03	1.18E+00	2.66E+01	9.4E-17	4.3E-01	6.2E-02	-0.8	0.01	-79.976	2804
1207-01C	670	2.85E+02	2.29E-01	9.12E-01	1.5E-14	2.2E+00	1.5E-02	5.3	0.81	18.328	2.804
1207-01E	800	5.98E+01	8.02E-02	1.12E-01	3.7E-14	6.4E+00	2.6E-02	44.7	2.88	32.129	0.356
1207-01F	900	3.66E+01	1.69E-02	2.80E-02	9.2E-14	3.0E+01	3.0E-02	77.3	7.97	33.935	0.103
1207-01H	1000	3.19E+01	7.14E-03	1.33E-02	2.9E-13	7.1E+01	3.2E-02	87.6	24.08	33.516	0.084
1207-01I	1100	3.06E+01	1.12E-02	8.64E-03	4.1E-13	4.6E+01	3.1E-02	91.6	46.76	33.655	0.053
1207-01J	1650	3.21E+01	4.03E-02	1.44E-02	9.6E-13	1.3E+01	3.1E-02	86.7	100.00	33.406	0.061
		total gas age	n=7		1.8E-12	3.0E+01	2.7E+01			33.353	0.239

Plateau Age (Steps F - J) = 33.58 ± 0.10

Run ID#	Temp	40/39	37/39	36/39	39K moles	K/Ca	Cl/K	%40*	%39Ar	Age	± Err
Sugarloaf Peak Quartz Monzonite Biotite											
VM 94-3; BIOT,4MG, J=0.0006713±0.000002											
1208-01B	650	8.32E+03	0.00E+00	2.80E+01	1.3E-16	#DIV/0!	3.9E-02	0.5	0.01	46.405	2462
1208-01C	700	1.25E+02	6.55E-02	3.33E-01	3.9E-14	7.8E+00	3.5E-02	21.0	2.18	31.437	0.535
1208-01E	800	3.62E+01	1.61E-02	2.85E-02	1.1E-13	3.2E+01	3.5E-02	76.7	8.41	33.297	0.104
1208-01F	900	2.95E+01	1.03E-02	6.80E-03	2.5E-13	5.0E+01	3.5E-02	93.1	22.33	32.976	0.074
1208-01G	1000	2.86E+01	1.01E-02	3.23E-03	3.6E-13	5.0E+01	3.5E-02	96.6	42.29	33.142	0.066
1208-01H	1100	2.88E+01	3.29E-02	3.75E-03	3.6E-13	1.5E+01	3.5E-02	96.1	62.52	33.156	0.061
1208-01I	1200	2.83E+01	6.96E-02	2.75E-03	6.2E-13	7.3E+00	3.7E-02	97.1	97.05	33.010	0.044
1208-0J	1650	2.91E+01	4.48E-02	5.23E-03	5.3E-14	1.1E+01	3.7E-02	94.6	#REF!	33.122	0.114
		total gas age		n=8	1.8E-12	#DIV/0!	#DIV/0!			33.049	0.249
Plateau Age (Steps F - I) = 33.063 ± 0.052											
Sugarloaf Peak Quartz Monzonite Hornblende											
VM 94-3; HBL,10MG, J=0.000675±0.000002											
1209-01B	800	7.68E+02	1.55E+00	2.45E+00	1.2E-14	3.3E-01	1.1E-01	5.7	5.98	52.860	9.020
1209-01C	900	2.77E+02	7.38E-01	8.44E-01	1.4E-14	6.9E-01	1.9E-02	9.8	12.72	32.699	2.983
1209-01D	950	1.11E+02	1.55E+00	2.77E-01	1.1E-14	3.3E-01	1.8E-02	26.1	18.21	34.943	0.976
1209-01E	1000	9.40E+01	4.82E+00	2.12E-01	1.2E-14	1.1E-01	7.3E-02	33.6	23.91	38.212	0.820
1209-01F	1030	1.54E+02	1.27E+01	3.75E-01	1.8E-14	4.0E-02	2.9E-01	28.4	32.48	52.892	1.052
1209-01G	1060	9.39E+01	1.48E+01	2.03E-01	2.7E-14	3.4E-02	3.7E-01	37.3	45.72	42.564	0.726
1209-01H	1100	4.24E+01	1.38E+01	5.12E-02	3.6E-14	3.7E-02	3.0E-01	66.7	63.40	34.430	0.283
1209-01I	1150	4.33E+01	1.05E+01	4.81E-02	2.9E-14	4.8E-02	2.3E-01	69.0	77.60	36.297	0.218
1209-0J	1200	5.02E+01	1.46E+01	4.38E-02	2.4E-14	3.5E-02	2.9E-01	76.4	89.40	46.629	0.340
1209-0K	1300	5.72E+01	1.76E+01	5.19E-02	1.7E-14	2.9E-02	3.6E-01	75.5	97.60	52.477	0.433
1209-0L	1650	6.69E+01	1.59E+01	1.33E-01	4.9E-15	3.2E-02	3.3E-01	43.2	100.00	35.228	1.217
		total gas age		n=11	2.1E-13	1.2E-01	2.1E-01			41.522	1.213
Quickstrike Mine K-feldspar											
QUICK 2; k-spar, 20.0 mg J=0.0006711±0.000002											
1210-01B	500	7.62E+02	5.12E-01	1.72E+00	1.6E-16	1.0E+00	8.3E-02	33.3	0.00	283.580	137.674
1210-01C	600	3.27E+02	1.07E-02	8.82E-01	9.0E-14	4.8E+01	2.9E-02	20.3	0.82	78.479	1.218

Run ID#	Temp	40/39	37/39	36/39	39K moles	K/Ca	Cl/K	%40*	%39Ar	Age	± Err
1210-01E	800	3.73E+01	2.81E-03	3.87E-02	6.9E-13	1.8E+02	1.9E-03	69.3	7.17	30.988	0.083
1210-01F	850	2.74E+01	0.00E+00	5.39E-03	2.6E-13	#DIV/0!	3.1E-04	94.1	9.58	30.948	0.056
1210-01G	900	2.67E+01	2.16E-04	2.19E-03	5.0E-13	2.4E+03	1.3E-04	97.5	14.15	31.211	0.054
1210-01H	950	2.68E+01	4.89E-04	3.15E-03	6.4E-13	1.0E+03	1.2E-04	96.4	20.03	31.010	0.050
1210-01I	1000	2.60E+01	3.24E-04	8.34E-04	5.9E-13	1.6E+03	1.5E-04	99.0	25.41	30.910	0.058
1210-01J	1050	2.59E+01	8.69E-04	1.08E-03	6.1E-13	5.9E+02	2.2E-04	98.7	30.99	30.715	0.047
1210-01K	1100	2.61E+01	6.31E-04	1.71E-03	5.9E-13	8.1E+02	3.4E-04	98.0	36.35	30.735	0.046
1210-01L	1150	2.67E+01	9.89E-04	3.65E-03	5.9E-13	5.2E+02	8.1E-04	95.9	41.71	30.731	0.042
1210-01M	1200	2.73E+01	8.66E-04	6.27E-03	6.1E-13	5.9E+02	1.1E-03	93.1	47.33	30.580	0.051
1210-01N	1250	2.83E+01	4.55E-04	7.01E-03	8.7E-13	1.1E+03	1.4E-03	92.6	55.28	31.445	0.038
1210-01O	1300	2.85E+01	6.24E-04	5.78E-03	1.6E-12	8.2E+02	1.0E-03	93.9	70.12	32.148	0.048
1210-01P	1650	2.90E+01	5.04E-03	7.02E-03	3.1E-12	1.0E+02	1.1E-03	92.8	98.24	32.300	0.046
1210-01Q	1650	2.88E+01	7.88E-03	7.57E-03	1.9E-13	6.5E+01	1.0E-03	92.2	100.00	31.837	0.222
		total gas age		n=15	1.1E-11	#DIV/0!	#DIV/0!			31.915	0.064

Sugarloaf Peak Quartz Monzonite K-feldspar
VM94-3; k-spar, 10.0 mg J=0.0006703±0.000002

1212-01C	450	2.85E+03	1.33E-01	6.87E+00	6.1E-15	3.8E+00	4.0E-01	28.9	0.06	793.397	34.396
1212-01F	550	1.29E+03	8.41E-02	2.40E+00	1.3E-14	6.1E+00	3.4E-01	44.8	0.19	588.934	8.463
1212-01I	600	1.57E+02	7.45E-02	3.13E-01	6.1E-14	6.8E+00	3.0E-02	41.2	0.77	76.764	0.551
1212-01L	700	1.32E+02	1.10E-01	2.42E-01	1.4E-13	4.6E+00	2.6E-02	45.8	2.10	71.460	0.382
1212-01N	800	3.98E+01	8.13E-02	3.07E-02	4.7E-13	6.3E+00	3.5E-03	77.2	6.61	36.803	0.121
1212-01O	850	2.94E+01	3.17E-02	6.83E-03	5.5E-13	1.6E+01	5.7E-04	93.1	11.95	32.786	0.051
1212-01P	900	2.93E+01	1.75E-02	6.60E-03	5.6E-13	2.9E+01	5.4E-04	93.3	17.40	32.789	0.052
1212-01Q	950	3.29E+01	1.86E-02	1.59E-02	5.2E-13	2.7E+01	1.2E-03	85.6	22.41	33.723	0.068
1212-01R	1000	2.98E+01	1.36E-02	8.11E-03	4.9E-13	3.8E+01	8.0E-04	91.9	27.15	32.810	0.049
1212-01S	1050	3.16E+01	1.58E-02	1.24E-02	5.0E-13	3.2E+01	1.6E-03	88.4	32.00	33.465	0.052
1212-01T	1050	3.21E+01	1.68E-02	1.25E-02	4.2E-13	3.0E+01	2.0E-03	88.5	36.08	34.070	0.055
1212-01U	1100	3.64E+01	2.23E-02	2.12E-02	4.6E-13	2.3E+01	3.9E-03	82.8	40.52	36.082	0.074
1212-01V	1100	3.64E+01	2.38E-02	2.02E-02	4.9E-13	2.1E+01	4.0E-03	83.5	45.22	36.450	0.069
1212-01W	1100	3.65E+01	2.40E-02	1.90E-02	4.2E-13	2.1E+01	3.8E-03	84.6	49.29	36.929	0.055
1212-01X	1100	3.56E+01	2.48E-02	1.48E-02	4.7E-13	2.1E+01	3.7E-03	87.7	53.85	37.302	0.052

Run ID#	Temp	40/39	37/39	36/39	39K moles	K/Ca	Cl/K	%40*	%39Ar	Age	± Err
1212-01Y	1100	3.48E+01	2.52E-02	1.20E-02	4.8E-13	2.0E+01	3.6E-03	89.8	58.51	37.380	0.063
1212-01Z	1100	3.53E+01	2.71E-02	1.15E-02	6.5E-13	1.9E+01	4.0E-03	90.3	64.84	38.142	0.058
1212-01ZA	1100	3.63E+01	2.91E-02	1.20E-02	6.7E-13	1.8E+01	3.9E-03	90.2	71.33	39.181	0.056
1212-01AA	1200	3.59E+01	1.58E-02	7.29E-03	5.8E-13	3.2E+01	4.5E-03	93.9	76.90	40.349	0.057
1212-01BB	1300	3.48E+01	1.21E-02	5.91E-03	1.4E-12	4.2E+01	3.3E-03	94.9	90.86	39.553	0.059
1212-01CC	1400	3.79E+01	3.17E-02	1.18E-02	3.2E-13	1.6E+01	5.0E-03	90.7	93.98	41.100	0.070
1212-01DD	1500	3.63E+01	2.44E-02	9.61E-03	5.4E-13	2.1E+01	3.8E-03	92.1	99.15	40.022	0.061
1212-01EE	1650	3.81E+01	1.43E-02	1.26E-02	8.7E-14	3.6E+01	4.8E-03	90.2	100.00	41.103	0.102
		total gas age		n=23	1.0E-11	2.5E+01	1.1E+01			38.757	0.100

D=	1.00600	4.00E-04
Ca 39/37=	0.00070	5.00E-05
Ca 36/37=	0.00026	2.00E-05
K 38/39=	0.01190	
K 40/39=	0.02200	1.00E-03

Hanover-Fierro K-feldspar

COB-4, Q5:17, K-spar, 18.1 mg, J=0.0007747±0.0000002

1848-01A	500	1.13E+03	1.12E-01	2.82E+00	8.4E-17	4.5E+00	6.9E-01	26.5	0.04	376.571	21.102
1848-01B	500	3.06E+02	0.00E+00	6.30E-01	9.1E-18	#DIV/0!	9.5E-02	39.2	0.05	160.224	40.196
1848-01C	575	3.57E+02	7.33E-02	7.20E-01	1.2E-16	7.0E+00	3.0E-01	40.4	0.11	191.185	4.387
1848-01D	575	7.70E+01	2.28E-02	8.52E-02	5.1E-17	2.2E+01	1.5E-02	67.3	0.13	71.037	3.247
1848-01E	650	1.02E+02	5.42E-02	1.23E-01	4.8E-16	9.4E+00	7.0E-02	64.4	0.37	89.684	0.704
1848-01F	650	5.44E+01	8.10E-02	1.75E-02	2.3E-16	6.3E+00	8.4E-03	90.4	0.49	67.461	0.745
1848-01G	725	6.21E+01	3.74E-02	3.58E-02	1.3E-15	1.4E+01	2.0E-02	82.9	1.15	70.542	0.272
1848-01H	725	4.70E+01	2.32E-02	1.24E-03	7.5E-16	2.2E+01	2.7E-03	99.2	1.52	63.961	0.313
1848-01I	800	4.65E+01	3.31E-02	6.66E-03	3.2E-15	1.5E+01	5.1E-03	95.7	3.10	61.191	0.151
1848-01J	800	4.28E+01	2.35E-02	1.41E-04	1.9E-15	2.2E+01	4.4E-04	99.9	4.03	58.817	0.156
1848-01K	875	4.27E+01	2.22E-02	2.05E-03	6.4E-15	2.3E+01	1.2E-03	98.5	7.26	57.811	0.122

Run ID#	Temp	40/39	37/39	36/39	39K moles	K/Ca	Cl/K	%40*	%39Ar	Age	± Err
1848-01L	875	4.16E+01	1.75E-02	-6.71E-04	3.7E-15	2.9E+01	1.6E-04	100.4	9.12	57.422	0.131
1848-01M	950	4.17E+01	1.78E-02	7.80E-04	9.7E-15	2.9E+01	2.8E-04	99.4	13.99	57.086	0.122
1848-01N	950	4.13E+01	1.55E-02	-3.06E-04	6.2E-15	3.3E+01	1.7E-05	100.2	17.11	56.917	0.122
1848-01O	1025	4.18E+01	1.20E-02	6.79E-04	1.3E-14	4.3E+01	1.7E-04	99.5	23.44	57.187	0.125
1848-01P	1025	4.14E+01	9.23E-03	-1.54E-04	7.0E-15	5.5E+01	-2.5E-04	100.1	26.93	56.942	0.117
1848-01Q	1100	4.15E+01	1.00E-02	3.92E-04	1.2E-14	5.1E+01	6.7E-05	99.7	33.07	56.972	0.118
1848-01R	1100	4.15E+01	7.56E-03	-7.57E-07	8.9E-15	6.7E+01	4.2E-06	100.0	37.53	57.066	0.119
1848-01S	1100	4.13E+01	6.93E-03	-1.44E-04	7.3E-15	7.4E+01	-1.3E-04	100.1	41.19	56.900	0.114
1848-01T	1100	4.16E+01	7.93E-03	1.18E-04	4.9E-15	6.4E+01	4.7E-04	99.9	43.64	57.134	0.120
1848-01U	1100	4.15E+01	6.90E-03	1.42E-04	3.9E-15	7.4E+01	-3.9E-05	99.9	45.59	57.050	0.132
1848-01V	1250	4.16E+01	1.14E-02	3.71E-04	1.6E-14	4.5E+01	4.2E-05	99.7	53.36	57.036	0.116
1848-01W	1300	4.23E+01	1.32E-02	1.58E-03	1.3E-14	3.9E+01	8.3E-04	98.9	59.92	57.452	0.124
1848-01X	1325	4.21E+01	1.65E-02	1.39E-03	1.3E-14	3.1E+01	1.1E-03	99.0	66.21	57.304	0.110
1848-02Y	1400	4.23E+01	1.76E-02	2.02E-03	2.1E-14	2.9E+01	1.3E-03	98.5	76.49	57.315	0.119
1848-02Z	1450	4.25E+01	1.70E-02	2.39E-03	2.3E-14	3.0E+01	1.3E-03	98.3	87.78	57.428	0.122
1848-02ZA	1550	4.26E+01	1.27E-02	2.67E-03	2.3E-14	4.0E+01	1.1E-03	98.1	99.21	57.482	0.127
1848-02ZB	1650	5.52E+01	1.95E-01	5.03E-02	1.6E-15	2.6E+00	3.2E-03	73.1	100.00	55.530	1.216
total gas age					2.0E-13				n=28	57.735	0.148

Granite Gap K-feldspar

GG, Q7:17, K-spar, 8.7 mg, J=0.0007768±0.0000002

1849-01A	500	1.35E+03	3.31E+00	4.75E+00	9.8E-18	1.5E-01	9.8E-02	-3.9	0.15	-74.949	157.597
1849-01B	500	1.09E+03	3.11E-01	2.96E+00	1.6E-17	1.6E+00	8.2E-02	19.5	0.41	274.743	61.738
1849-01C	575	7.08E+02	2.11E-01	1.59E+00	2.2E-17	2.4E+00	9.6E-02	33.7	0.75	306.582	25.770
1849-01D	575	3.09E+02	4.95E-01	9.45E-01	3.5E-17	1.0E+00	5.4E-02	9.6	1.30	41.309	11.978
1849-01E	650	2.25E+02	7.85E-01	5.62E-01	3.6E-17	6.5E-01	3.3E-02	26.3	1.85	81.179	8.072
1849-01F	650	5.59E+01	8.35E-01	1.36E-01	7.9E-17	6.1E-01	1.9E-02	28.3	3.08	22.060	2.560
1849-01G	725	6.61E+01	1.09E+00	9.52E-02	1.1E-16	4.7E-01	1.4E-02	57.6	4.71	52.635	1.646
1849-01H	725	2.27E+01	1.14E+00	2.46E-02	1.5E-16	4.5E-01	6.8E-03	68.2	7.08	21.603	1.109
1849-01I	800	1.75E+02	0.00E+00	7.88E-02	1.7E-18	#DIV/0!	5.2E-02	86.7	7.11	201.412	116.456
1849-01J	800	1.57E+02	0.00E+00	5.96E-01	1.1E-17	#DIV/0!	-7.0E-02	-12.1	7.27	-26.883	42.687

Run ID#	Temp	40/39	37/39	36/39	39K moles	K/Ca	Cl/K	%40*	%39Ar	Age	± Err
1849-01K	875	2.71E+01	3.74E-01	6.93E-02	-2.1E-17	1.4E+00	1.4E-02	24.4	6.94	9.239	9.502
1849-01L	875	2.72E+01	8.21E-01	2.04E-02	1.3E-16	6.2E-01	2.6E-03	78.0	8.99	29.510	1.436
1849-01M	950	2.21E+01	4.15E-01	4.31E-03	1.6E-16	1.2E+00	-1.1E-03	94.3	11.50	28.943	1.196
1849-01N	950	2.47E+01	2.44E-01	1.18E-02	4.0E-16	2.1E+00	-1.3E-04	85.9	17.74	29.465	0.538
1849-01O	1025	2.23E+01	1.02E-01	5.76E-04	3.8E-16	5.0E+00	-3.6E-04	99.2	23.59	30.724	0.521
1849-01P	1025	2.40E+01	5.06E-02	6.05E-03	6.2E-16	1.0E+01	2.8E-06	92.5	33.30	30.861	0.351
1849-01Q	1100	2.32E+01	6.24E-02	2.57E-03	1.1E-15	8.2E+00	2.9E-04	96.7	50.90	31.108	0.169
1849-01R	1100	3.02E+01	3.10E-02	2.74E-02	4.7E-16	1.6E+01	-8.1E-04	73.2	58.16	30.721	0.431
1849-01S	1100	5.22E+01	4.59E-02	1.03E-01	2.6E-16	1.1E+01	-3.8E-04	41.8	62.14	30.306	0.892
1849-01T	1100	8.64E+01	1.67E-01	2.13E-01	2.0E-16	3.1E+00	8.6E-04	27.3	65.20	32.698	1.348
1849-01U	1200	2.53E+01	5.15E-01	-1.77E-02	7.6E-17	9.9E-01	3.7E-03	120.8	66.38	42.317	2.096
1849-01V	1275	2.07E+01	4.06E+00	1.98E-02	2.0E-16	1.3E-01	1.8E-02	73.1	69.44	21.154	2.653
1849-01W	1349	2.78E+01	2.05E+00	1.61E-02	3.5E-16	2.5E-01	1.4E-03	83.4	74.93	32.274	0.448
1849-01X	1450	3.94E+01	2.99E-01	3.83E-02	8.1E-16	1.7E+00	8.9E-04	71.3	87.59	38.900	0.263
1849-01Y	1650	8.41E+01	4.25E-01	1.99E-01	8.0E-16	1.2E+00	1.7E-03	30.1	100.00	35.162	2.484
total gas age					6.4E-15				n=25	34.014	1.519

Granite Gap biotit

GG, Q8:17, biotite, 19.4 mg, J=0.0007821±0.0000002

1850-01IA	650	1.56E+02	6.33E-02	4.36E-01	3.0E-16	8.1E+00	4.5E-02	17.7	0.52	38.593	1.872
1850-01IB	730	9.15E+01	0.00E+00	2.12E-01	2.9E-16	#DIV/0!	1.0E-02	31.5	1.03	40.142	1.059
1850-01IC	780	6.10E+01	7.12E-03	1.22E-01	8.6E-16	7.2E+01	6.3E-03	41.0	2.53	34.955	0.443
1850-01ID	830	3.87E+01	9.07E-03	4.84E-02	1.3E-15	5.6E+01	5.3E-03	63.0	4.73	34.072	0.277
1850-01IE	860	3.04E+01	1.09E-02	1.99E-02	1.5E-15	4.7E+01	4.6E-03	80.6	7.32	34.238	0.177
1850-01IF	900	2.75E+01	8.96E-03	8.94E-03	2.1E-15	5.7E+01	4.4E-03	90.3	11.05	34.651	0.121
1850-01IG	950	2.61E+01	7.59E-03	5.96E-03	3.6E-15	6.7E+01	4.4E-03	93.2	17.31	33.981	0.094
1850-01IH	1000	2.65E+01	8.71E-03	7.85E-03	4.1E-15	5.9E+01	4.3E-03	91.2	24.45	33.764	0.104
1850-01II	1100	2.62E+01	1.12E-02	7.76E-03	7.0E-15	4.6E+01	3.7E-03	91.2	36.83	33.361	0.096
1850-01IJ	1200	2.69E+01	3.77E-01	1.15E-02	6.5E-15	1.4E+00	4.3E-03	87.3	48.29	32.800	0.100
1850-01IK	1300	2.49E+01	6.05E-02	4.23E-03	1.8E-14	8.4E+00	4.8E-03	94.9	80.63	32.992	0.080
1850-01IL	1650	2.64E+01	2.36E-01	1.02E-02	1.1E-14	2.2E+00	3.5E-03	88.6	100.00	32.738	0.095
total gas age					5.7E-14				n=12	33.296	0.118

Run ID#	Temp	40/39	37/39	36/39	39K moles	K/Ca	Cl/K	%40*	%39Ar	Age	± Err
Plateau age (Steps G-L) = 33.2 ± 0.2											

Hanover-Fierro biotite

COB-4, Q8:17, biotite, 18.5 mg, J=0.0007945±0.0000002

1851-01A	650	1.43E+02	2.10E-01	3.33E-01	5.5E-16	2.4E+00	4.0E-02	31.1	0.35	62.532	1.132
1851-01B	800	4.48E+01	2.01E-01	1.48E-02	3.3E-15	2.5E+00	1.2E-02	90.2	2.45	57.078	0.158
1851-01C	900	4.18E+01	2.93E-02	4.81E-03	1.1E-14	1.7E+01	2.0E-02	96.6	9.25	56.933	0.129
1851-01D	1000	4.08E+01	9.11E-03	2.73E-05	2.0E-14	5.6E+01	2.3E-02	99.9	21.59	57.450	0.119
1851-01E	1075	4.07E+01	7.32E-03	-2.99E-05	1.9E-14	7.0E+01	2.3E-02	100.0	33.70	57.386	0.127
1851-01F	1150	4.09E+01	7.17E-03	1.55E-05	1.8E-14	7.1E+01	2.3E-02	99.9	44.78	57.701	0.123
1851-01G	1200	4.09E+01	1.14E-02	8.57E-05	1.7E-14	4.5E+01	2.3E-02	99.9	55.24	57.597	0.127
1851-01H	1250	4.09E+01	2.34E-02	1.84E-04	1.5E-14	2.2E+01	2.3E-02	99.8	64.59	57.638	0.123
1851-01I	1100	4.12E+01	0.00E+00	7.21E-04	1.2E-15	#DIV/0!	2.4E-02	99.4	65.35	57.726	0.196
1851-01J	1300	4.08E+01	2.14E-02	1.70E-04	2.5E-14	2.4E+01	2.6E-02	99.8	81.01	57.454	0.119
1851-01K	1400	4.09E+01	3.52E-02	4.20E-04	2.6E-14	1.4E+01	2.6E-02	99.7	97.41	57.516	0.165
1851-01L	1650	4.32E+01	4.71E-01	1.11E-02	4.1E-15	1.1E+00	8.7E-03	92.4	100.00	56.305	0.480
total gas age					1.6E-13				n=12	57.462	0.144

Plateau age (Steps G - J) = 57.03 ± 0.05

D=	1.01E+00	1.60E-03
Ca 39/37=	7.00E-04	5.00E-05
Ca 36/37=	2.60E-04	2.00E-05
K 38/39=	1.19E-02	
K 40/39=	1.90E-02	2.00E-03

1—Location of areas of study in southwestern New Mexico.

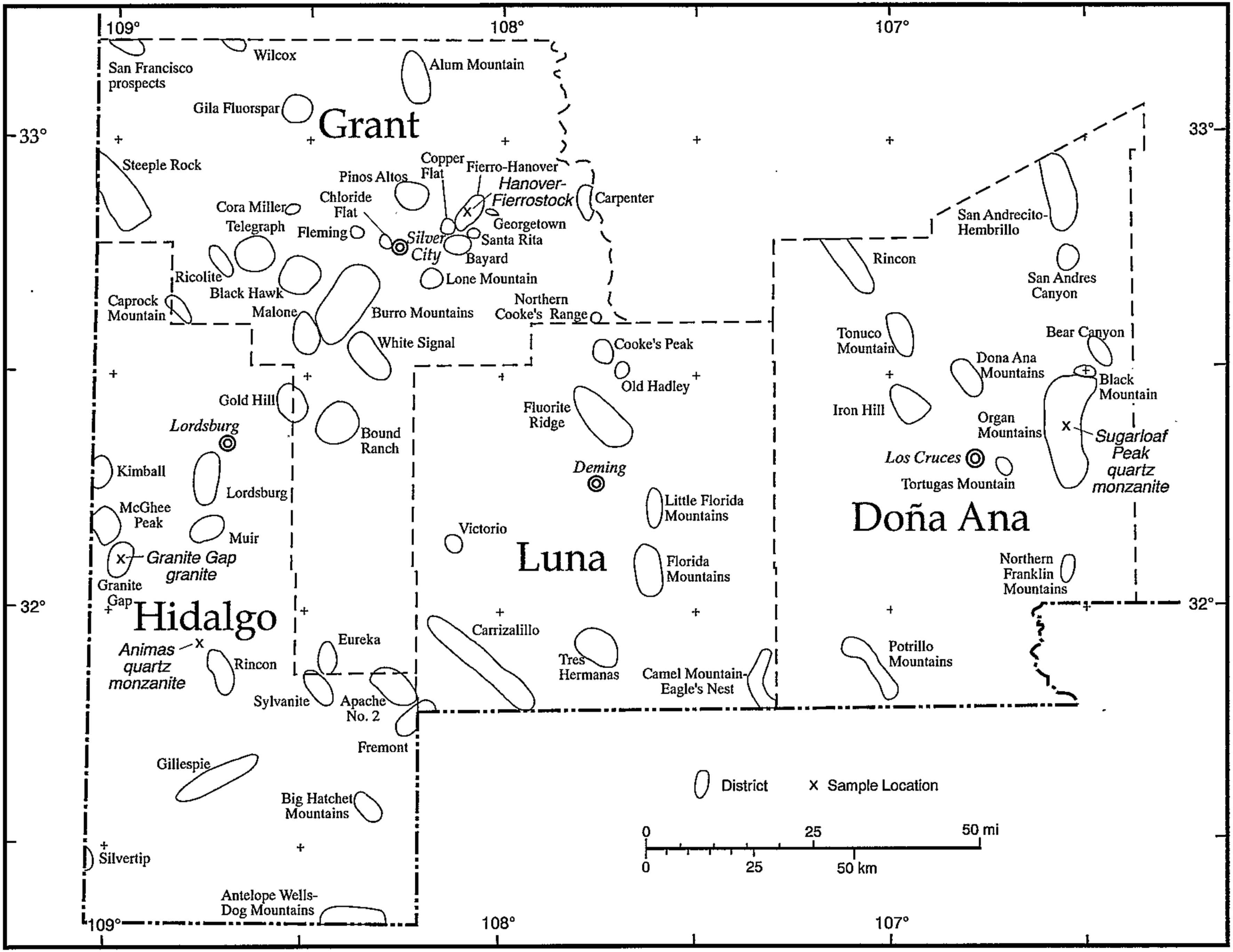

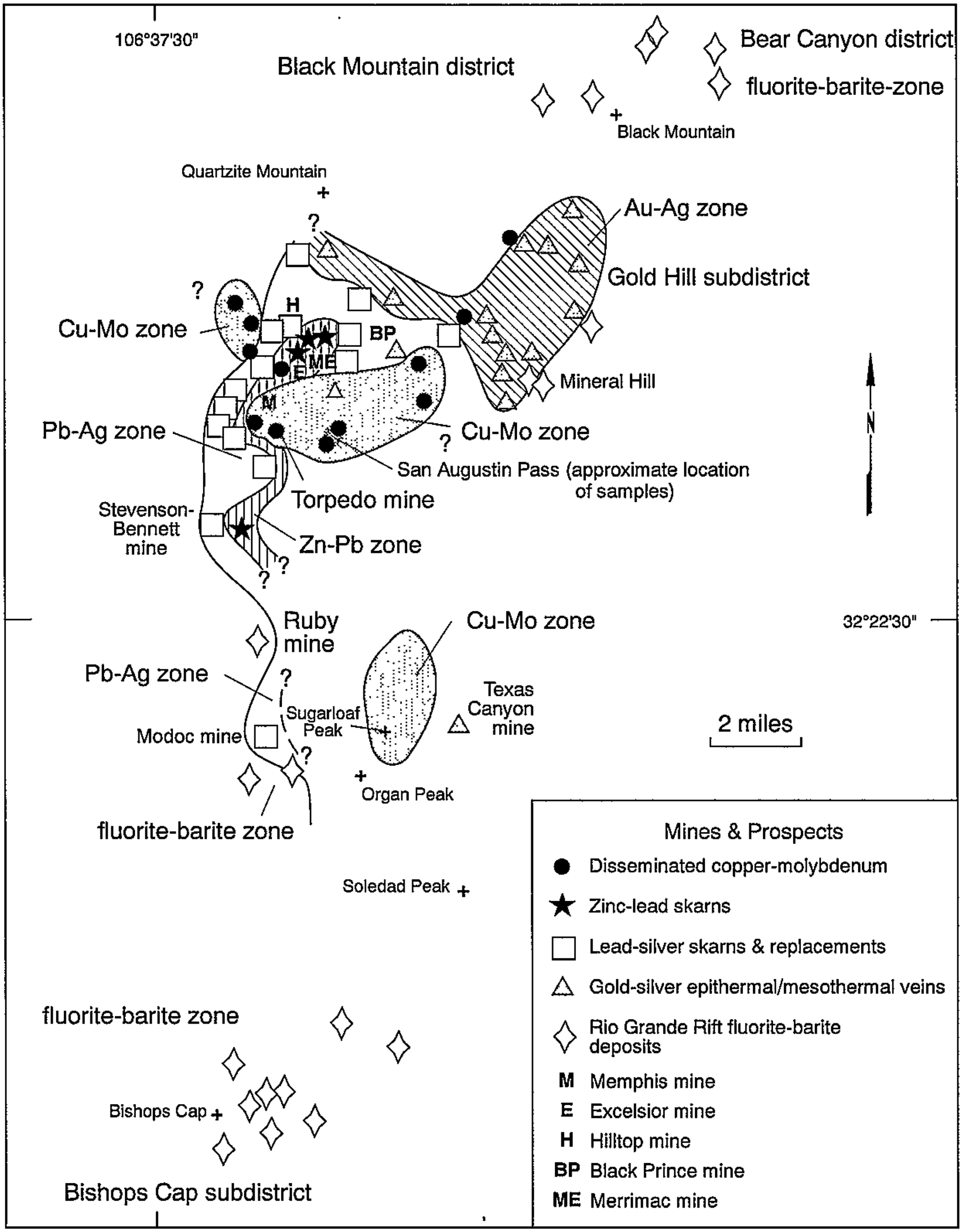

2—District zoning in the Organ Mountains, Doña Ana County, New Mexico (modified from Dunham, 1935; Seager, 1981).

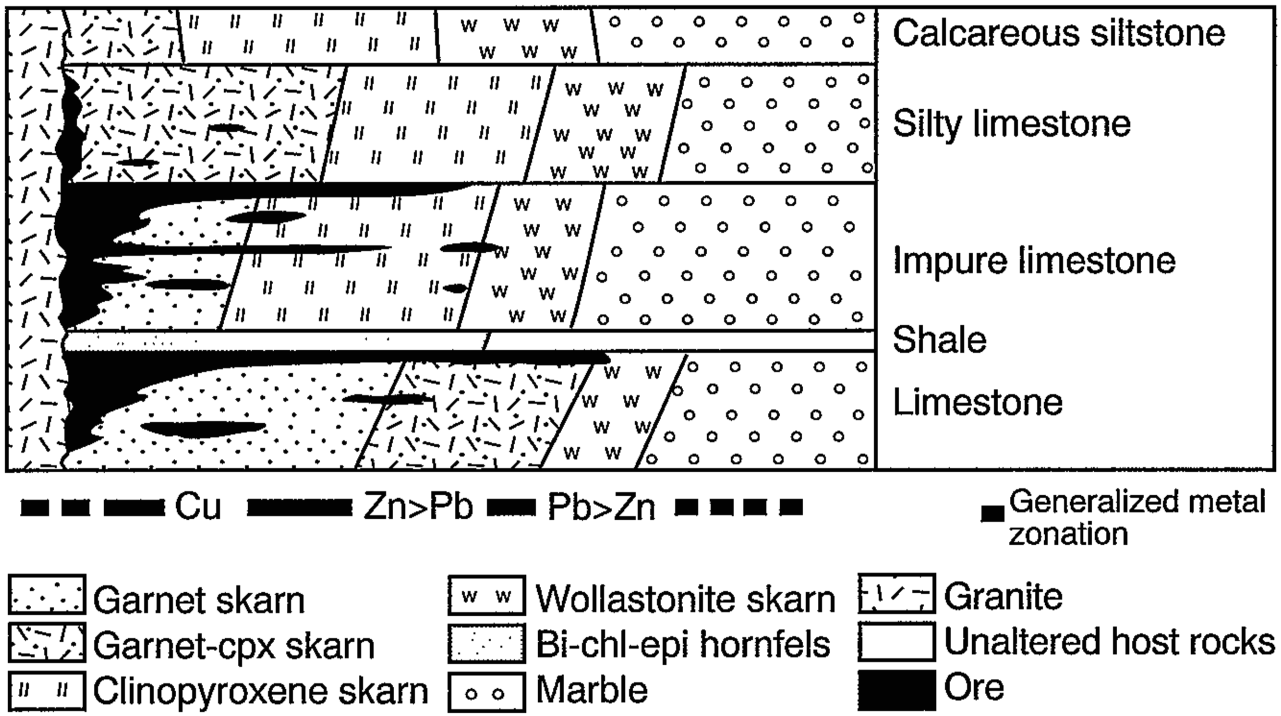

3—Generalized mineral zoning in Laramide skarn deposits in the Fierro–Hanover district (modified from Lueth, 1984). Garnet with chalcopyrite forms nearest to the stock in the purer limestones and garnet–clinopyroxene forms adjacent to the stock in the argillaceous carbonate rocks. Lead–zinc forms in more distal zones from the igneous contact.

4 - Spectra of Animas biotite

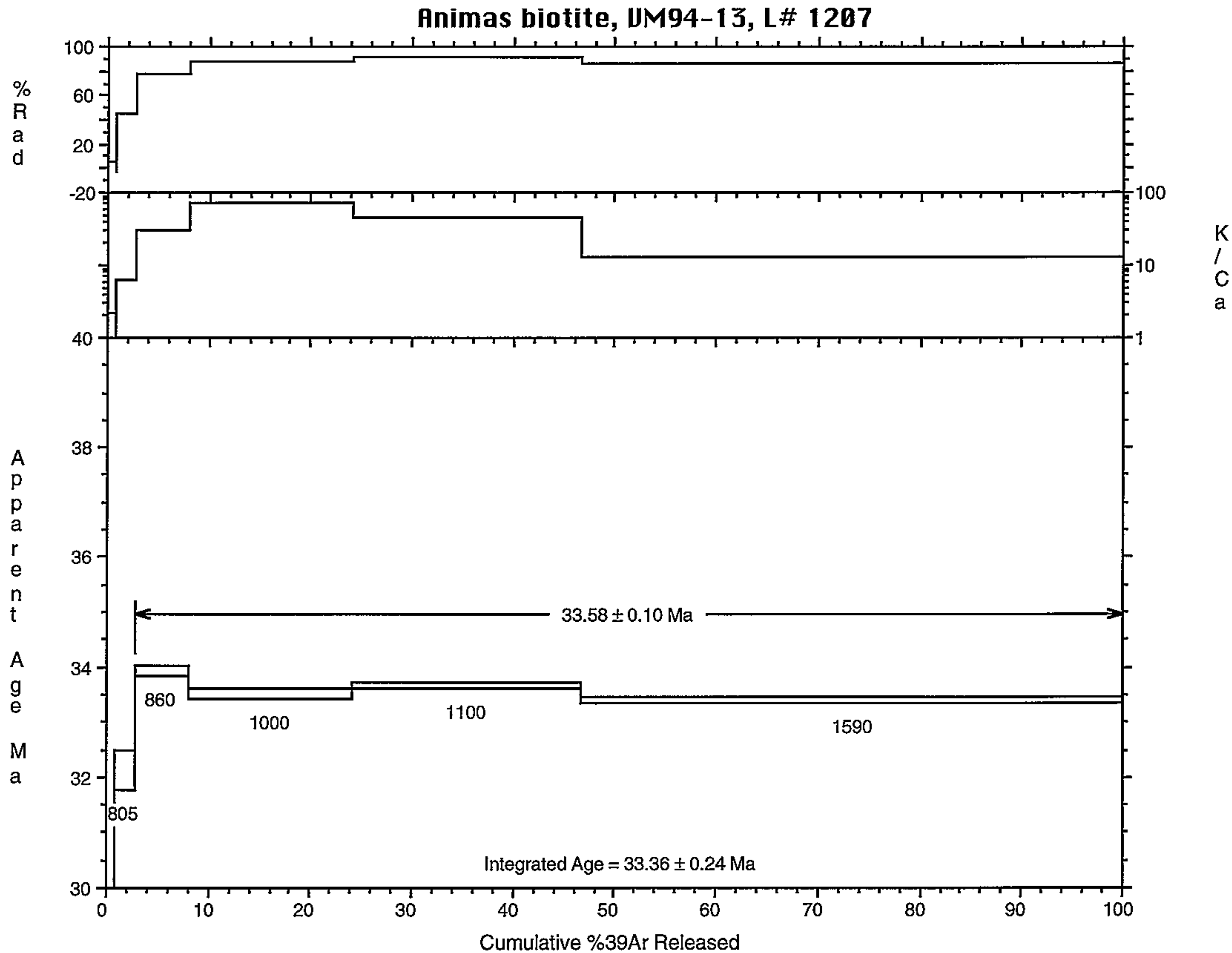

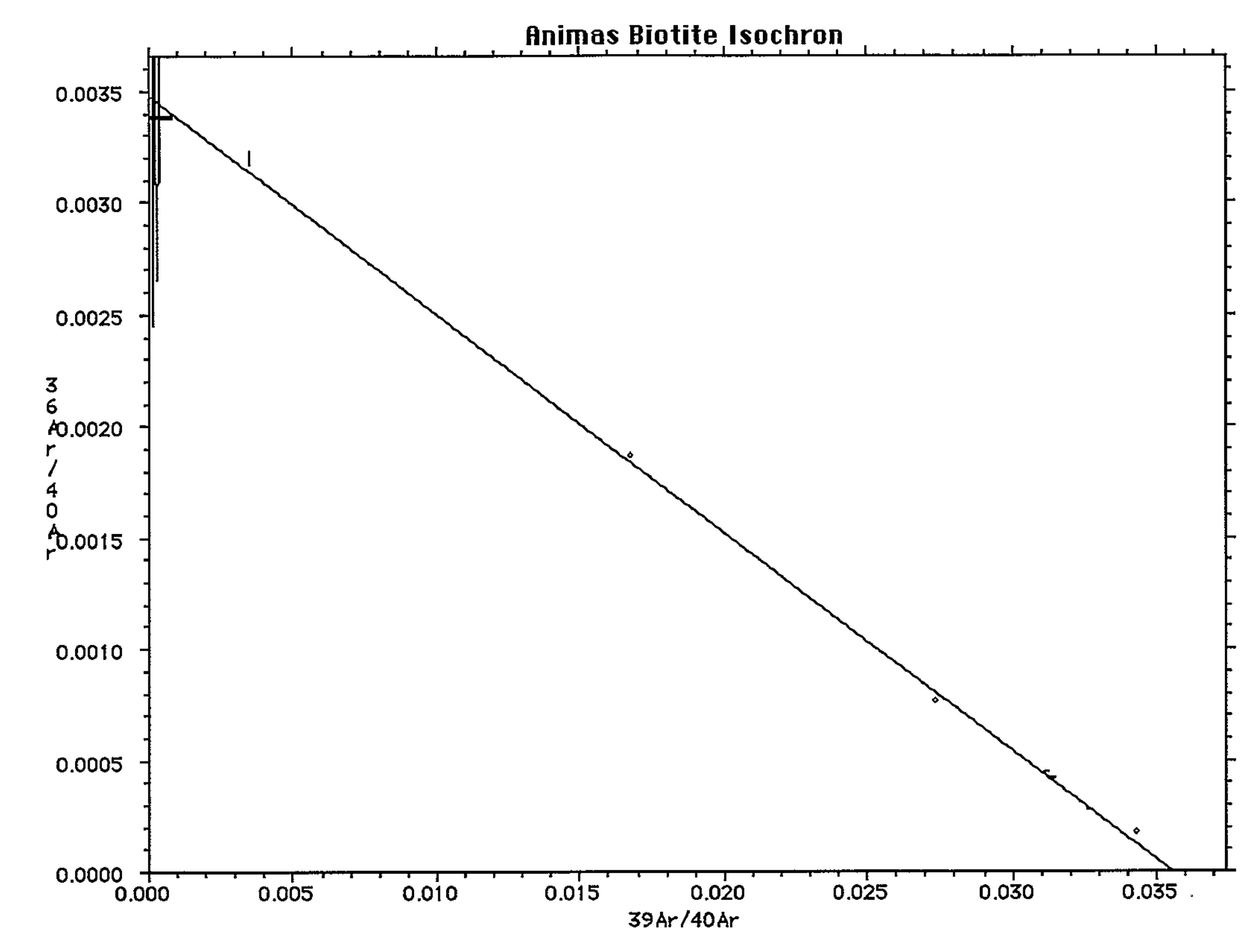

5— Isochron of Animas biotite.

6 - Spectra of Sugarloaf Peak biotite

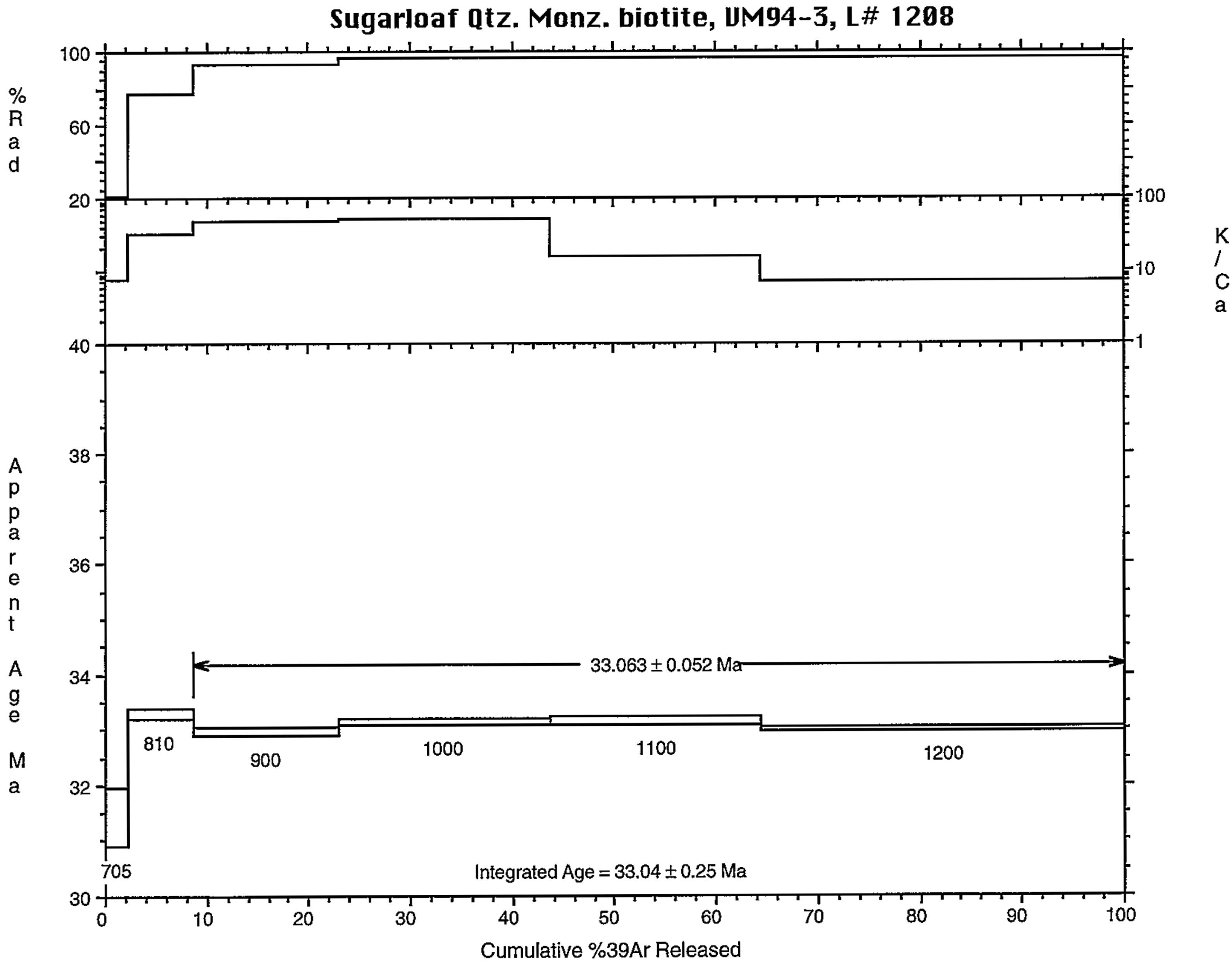

7 - Spectra of Sugarloaf Peak feldspar

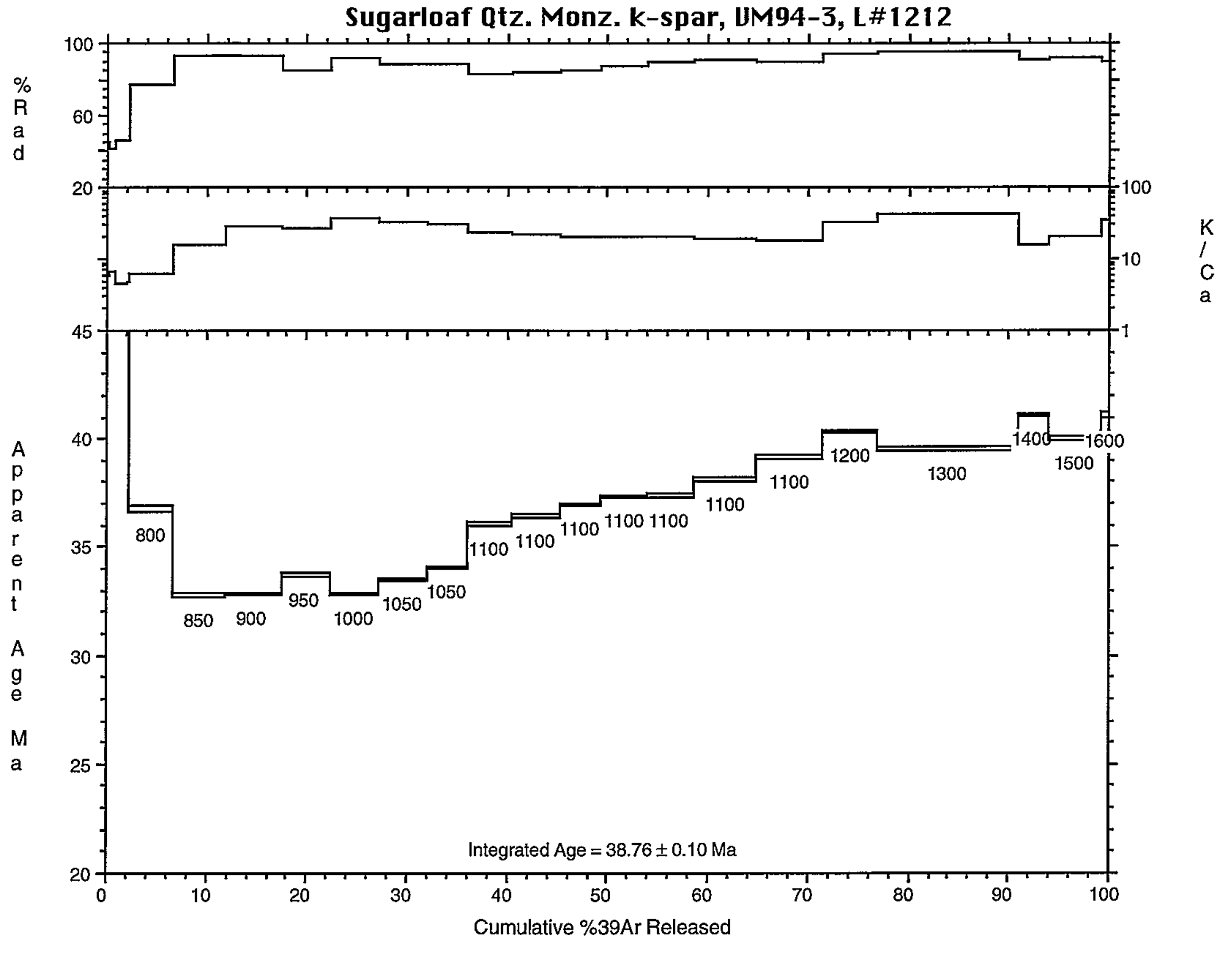

8 - Spectra of Sugarloaf Peak Hornblende

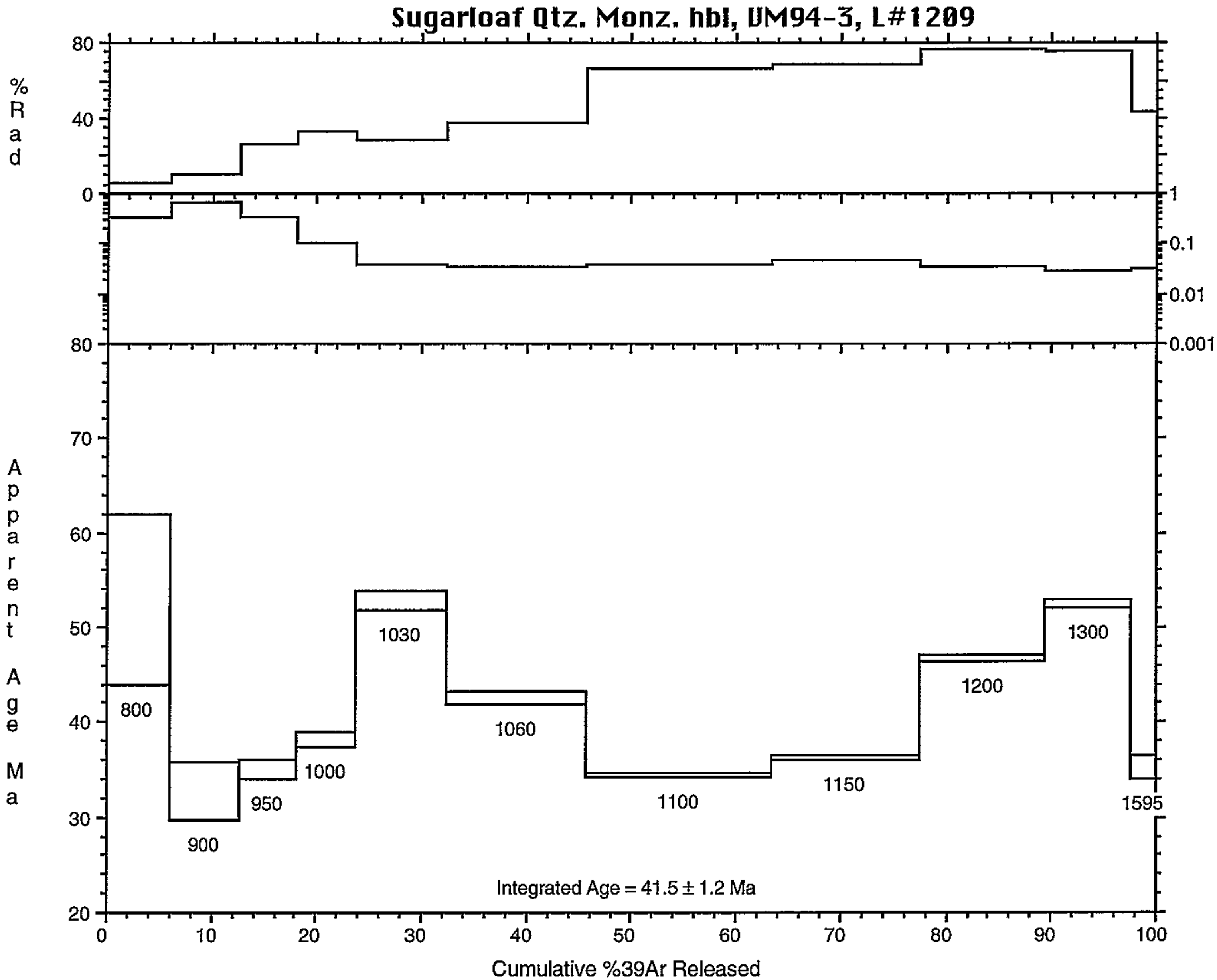

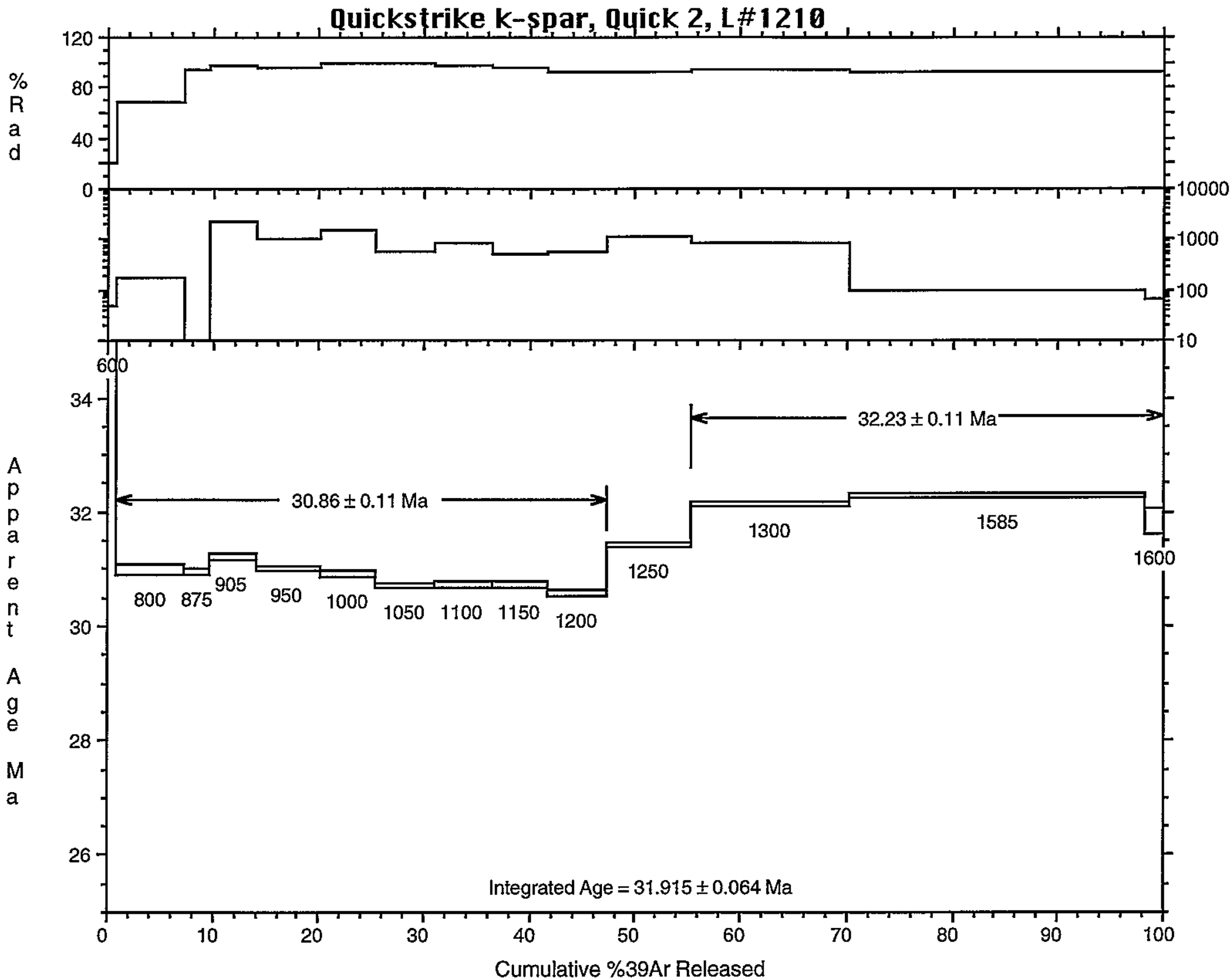

9 - Spectra of Quickstrike K-feldspar

10 - Spectra of Hanover-Fierro biotite

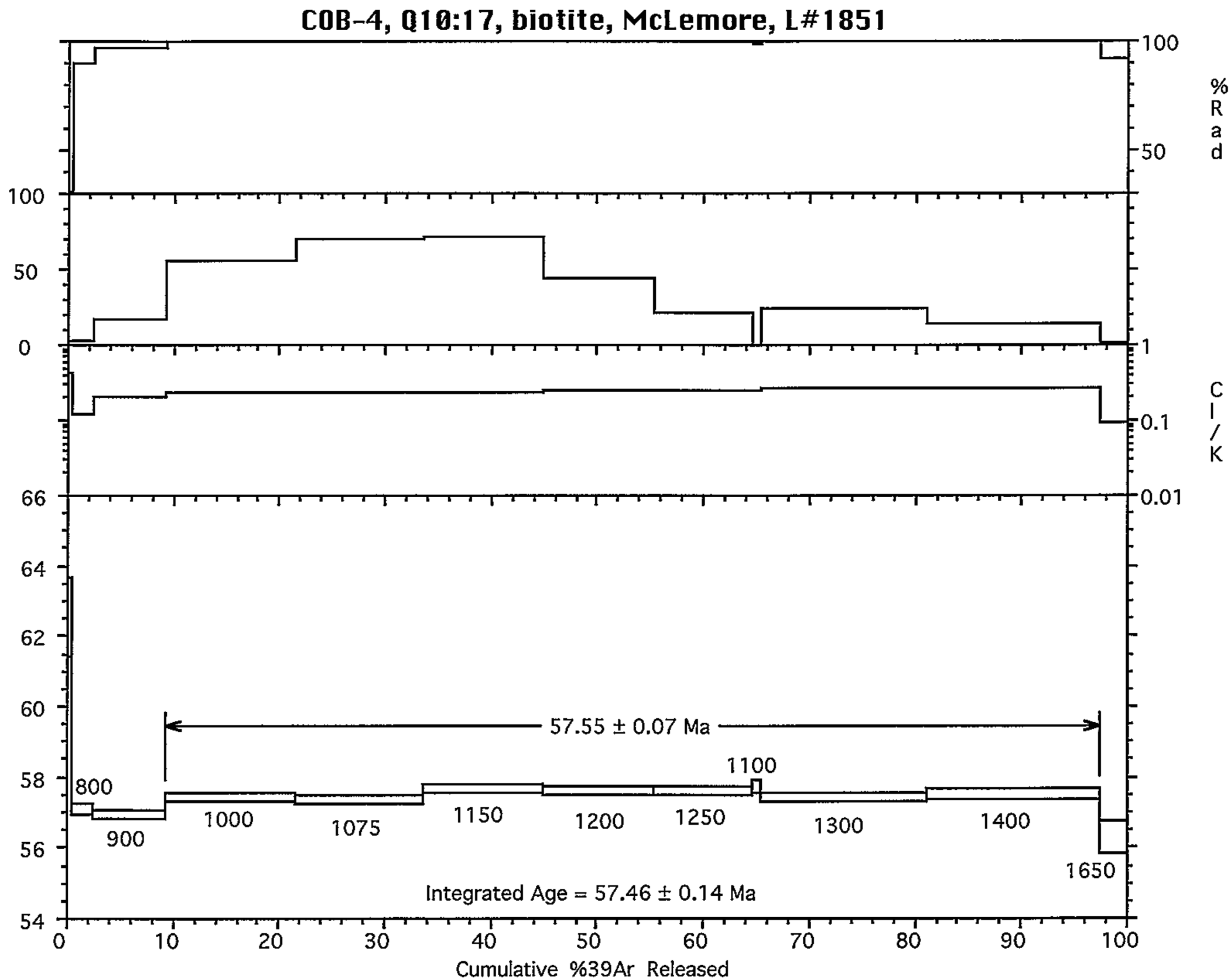

11 - Isochron of Hanover-Fierro biotite

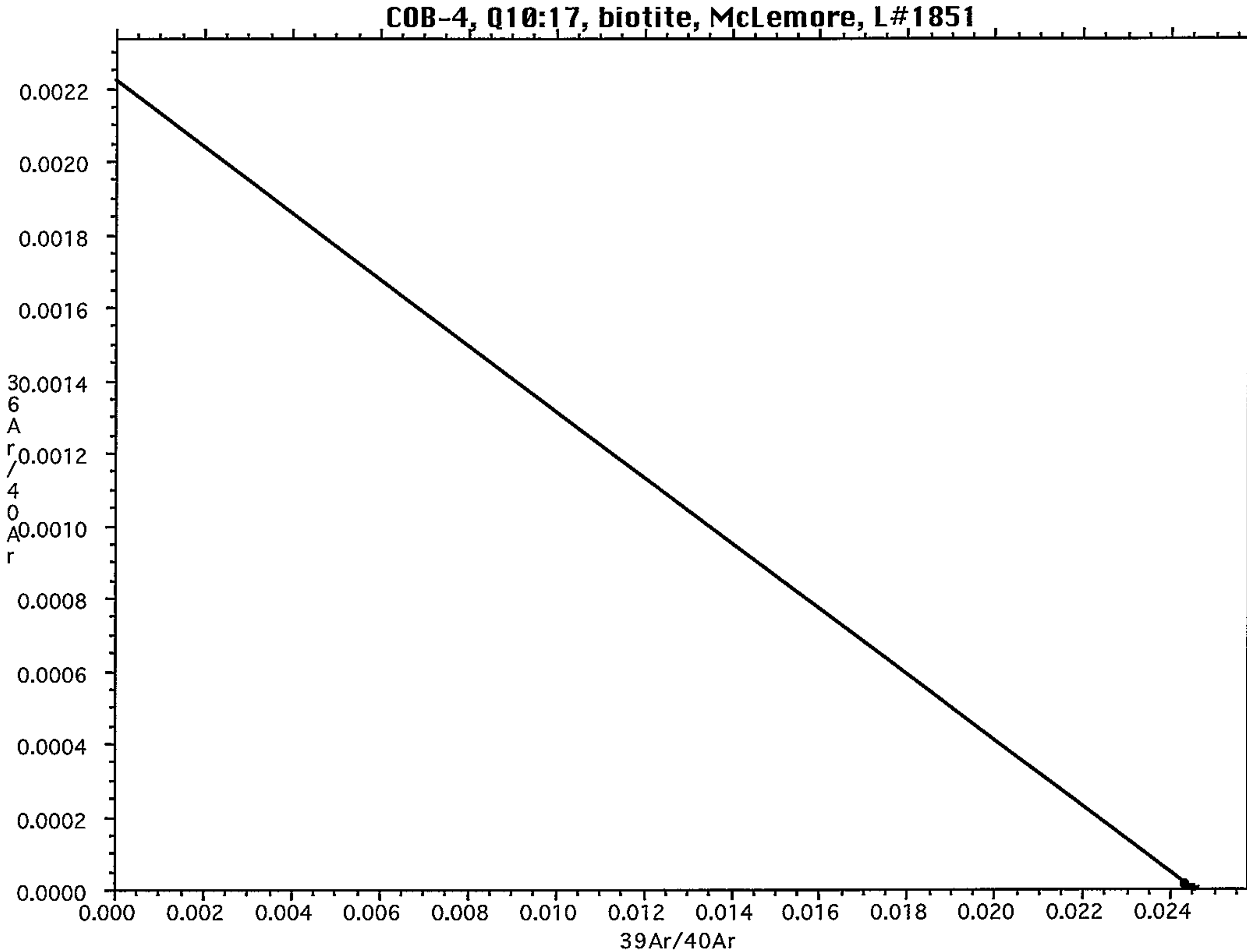

12 - Spectra of Hanover-Fierro K-Feldspar

COB-4, Q5:17, Kspar, McLemore, L#1848

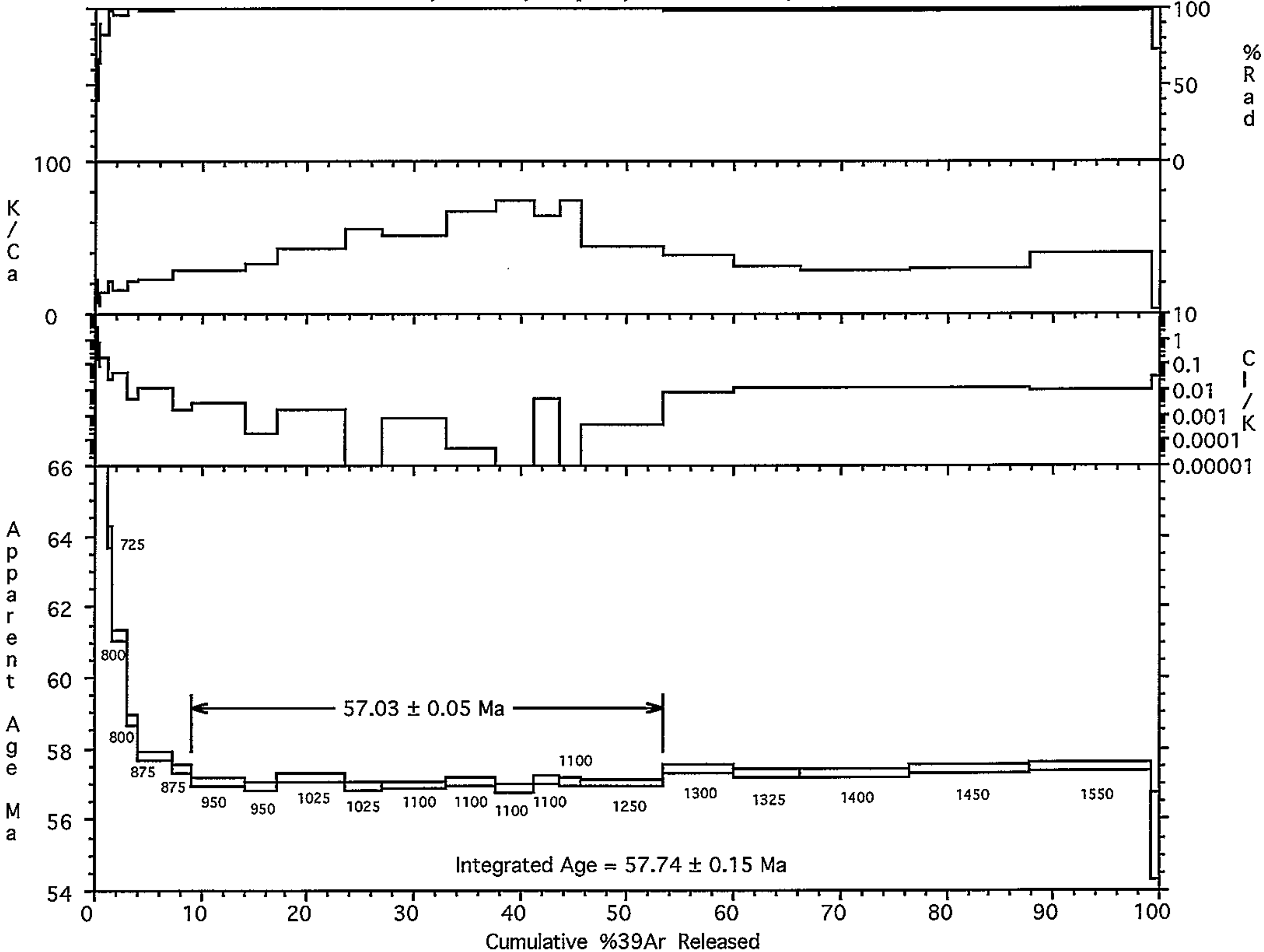

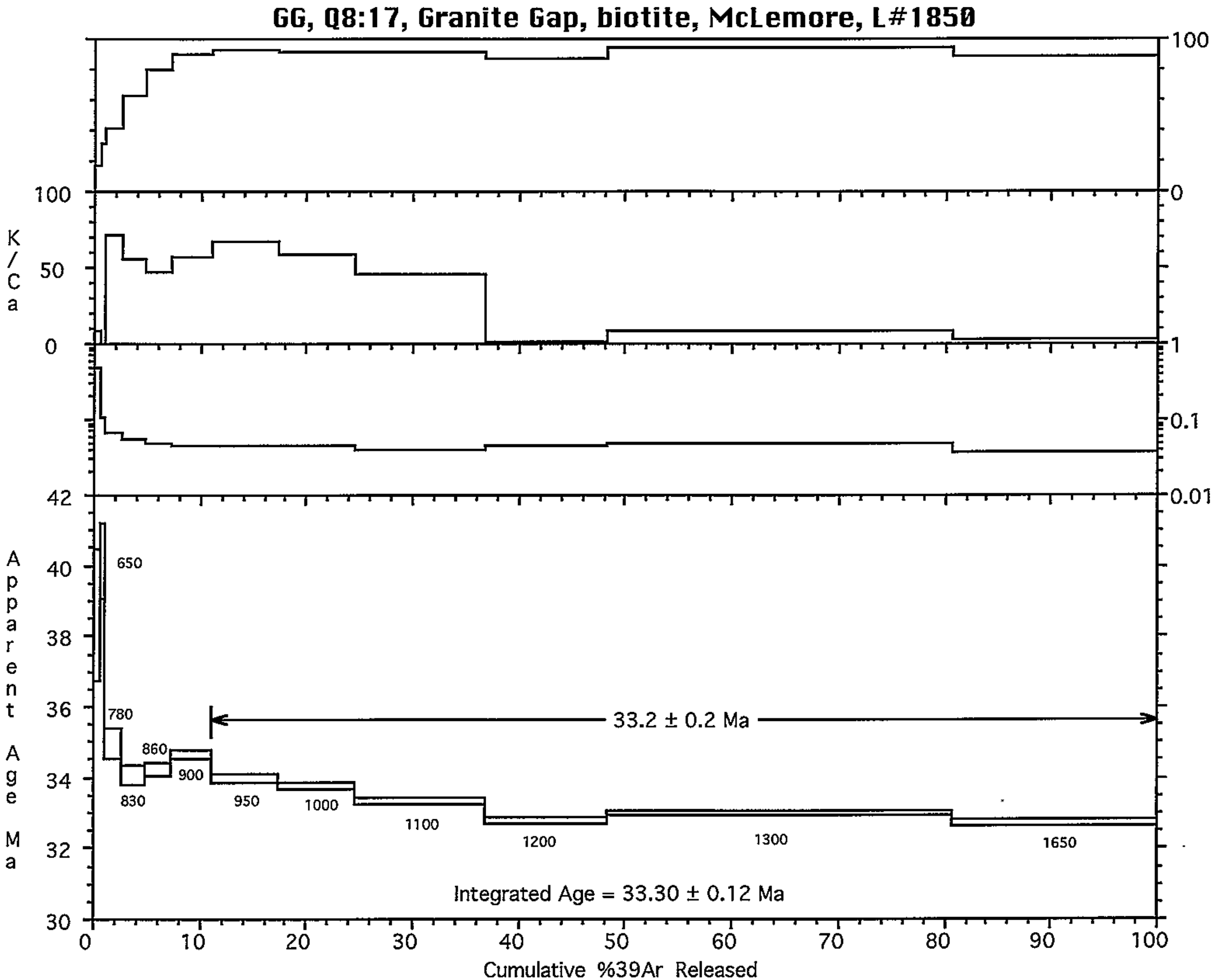

13 - Spectra of Granite Gap biotite

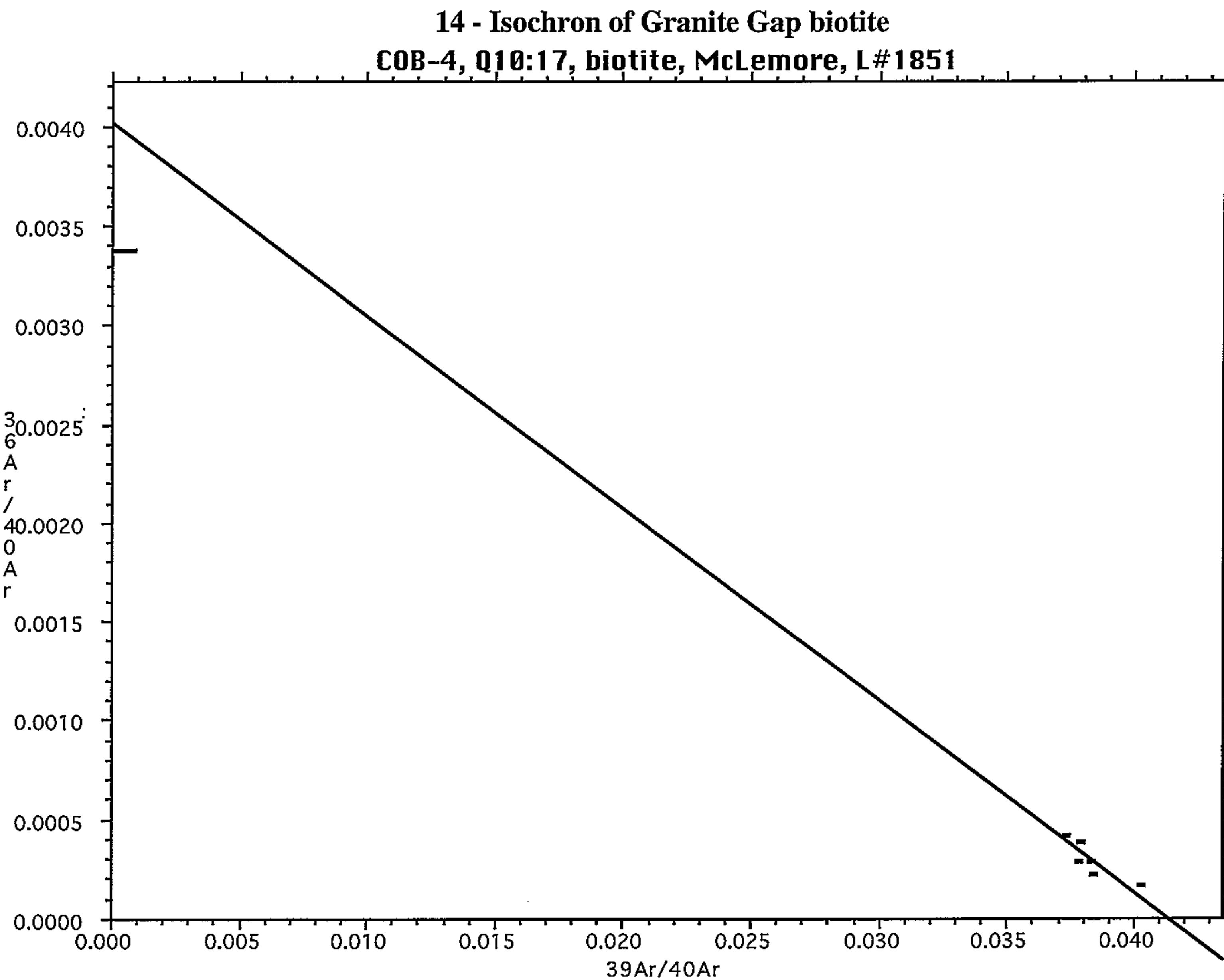
14 - Isochron of Granite Gap biotite
COB-4, Q10:17, biotite, McLemore, L#1851
0.0040
0.0035
0.0030
0.0025
0.0020
0.0015
0.0010
0.0005
0.0000
36Ar/40Ar
0.000
0.005
0.010
0.015
0.020
0.025
0.030
0.035
0.040
39Ar/40Ar

15 - Spectra of Granite Gap K-feldspar

GG, Q7:17, Granite Gap, feldspar?, McLemore, L#1849